Electronic Thesis and Dissertation Repository

8-21-2014 12:00 AM

The Role of the Pre-Sensor 1 **β** Hairpin in Minichromosome Maintenance 2-7 Function

Simon K. W. Lam
The University of Western Ontario

Supervisor
Christopher J Brandl
The University of Western Ontario

Graduate Program in Biochemistry
A thesis submitted in partial fulfillment of the requirements for the degree in Master of Science
© Simon K. W. Lam 2014

Follow this and additional works at: https://ir.lib.uwo.ca/etd

 Part of the Biochemistry Commons, Molecular Biology Commons, and the Structural Biology Commons

Recommended Citation
Lam, Simon K. W., "The Role of the Pre-Sensor 1 β Hairpin in Minichromosome Maintenance 2-7 Function" (2014). *Electronic Thesis and Dissertation Repository*. 2374.
https://ir.lib.uwo.ca/etd/2374

THE ROLE OF THE PRE-SENSOR 1 β HAIRPIN IN MINICHROMOSOME MAINTENANCE 2-7 FUNCTION.

(Thesis format: Integrated-Article)

by

Simon, <u>Lam</u>

Graduate Program in Biochemistry

A thesis submitted in partial fulfillment
of the requirements for the degree of
Master of Science

The School of Graduate and Postdoctoral Studies
The University of Western Ontario
London, Ontario, Canada

ABSTRACT

The pre-sensor 1 (PS1) β hairpin is found in helicases of the AAA+ family (**A**TPases **a**ssociated with a variety of cellular **a**ctivities) of proteins and is implicated in DNA translocation during DNA unwinding. To determine whether the PS1 β hairpin is required in the eukaryotic replicative helicase, Mcm2-7 (also comprised of AAA+ proteins), we mutated the conserved lysine residue in the PS1 β hairpin in each of the *S. cerevisiae* Mcm subunits to alanine. Only the PS1 β hairpin of Mcm3 was essential for viability, while mutation of the PS1 β hairpin in the remaining Mcm subunits resulted in minimal phenotypes, with the exception of Mcm7. The viable alleles were synthetic lethal with each other. Mcm2-7 containing $Mcm3_{K499A}$ ($Mcm2-7_{3K499A}$) disrupts helicase activity, yet the ATPase activity of $Mcm2-7_{3K499A}$ was similar to the wild type Mcm2-7, and its interaction with single-stranded DNA was subtly altered *in vitro*. These findings indicate that the PS1 β hairpins in the Mcm2-7 subunits have important and distinct functions most evident with $Mcm3_{K499A}$.

CO-AUTHORSHIP STATEMENT

The majority of the experimental work presented in this thesis was performed by myself. Dr. Christopher J Brandl performed tetrad dissection and Dr. Brian Shilton generated the Mcm2-7 models presented in Chapters 1 and 2 of this thesis. I supplied and prepared the materials for the gel filtration experiment, which was performed by Xiaoli Ma. The electrophoretic mobility DNA shift assay was optimized by Xiaoli Ma that is presented in this thesis. The *MCM2* and *MCM7* plasmids were cloned by Tina Sing.

ACKNOWLEDGMENTS

I would like to express my sincerest gratitude to all the friends I have made in the biochemistry department, especially the Davey lab members, Lance DaSilva, Tom Kolaczyk, Gillian Lazarovitz, Mike Ellis, and Matt Renaud who have always kept the lab such a fun place to conduct research. I could always count on you to make me laugh even in the face of adversity when experiments fail or when experiments succeed.

I would like to thank Roseline Godbout at the Cross Cancer Institute who gave me the first research opportunity. Even though I am no longer mucking about in your lab you have always been providing me valuable and thoughtful advice throughout the years in regards to my career and schooling.

I appreciate all the guidance and support I have received from my mentor, Megan Davey. In addition to being such a remarkable scientist, you provided me such a wonderful environment to flourish as a grad student. I have learned so much about research, life, resilience, and wittiness from you.

Most importantly, I would like to thank my parents Billy and Julie Lam, my brother, Albert Lam, and my sister-in-law, Christine Lam for all their unconditional support and infinite patience as I pursued my research.

TABLE OF CONTENTS

LIST OF TABLES

Table:

LIST OF FIGURES

Chapter 1 Figures:

Chapter 2 Figures:

LIST OF ABBREVIATIONS AND SYMBOLS

AAA+	**A**TPases **A**ssociated with diverse cellular **A**ctivities
ADP	Adenosine Diphosphate
ATP	Adenosine Triphosphate

Amino Acids

A	Alanine
N	Asparagine
Q	Glutamine
K	Lysine
R	Arginine

α	alpha
β	beta
γ	gamma
μ	micro
Å	Angstrom
°C	Degree Celsius
[γ^{32}P] ATP	radiolabeled gamma phosphate of Adenosine Triphosphate
μC	microcurie
μm	micrometre
Cdc	Cell division control
Cdc7	Cell division control 7
Cdc45	Cell division control 45
Cdk	Cyclin dependent kinase

Cdt1	Cdc10-dependent transcript 1
CEN	centromeric DNA sequence
C-terminal	carboxy terminal
Dbf4	Dumbbell former protein 4
DDK	Dbf4 Dependent Kinase
DTT	Dithiothreitol
DNA	Deoxyribonucleic Acid
dsDNA	double stranded Deoxyribonucleic Acid
E1	Bovine Papillomavirus E1
E. coli	*Escherichia coli*
EDTA	Ethylene-Diamine-Tetra-Acetic acid
Ext	External
G1	Gap Phase 1
G2	Gap Phase 2
GAL	galactose metabolism gene
H2I	Helix 2 Insert
HCl	Hydrochloric acid
HEPES	4-(2-hydroxyethyl)-1-piperazineethanesulfonic acid
HU	Hydroxyurea
LB	Luria-Bertani
LEU2	gene encodes for beta-isopropylmalate dehydrogenase (leucine biosynthesis enzyme)
M	Mitosis

mCi	millicurie
MCM	Minichromosome maintenance
mec2-1	gene encoding for Rad53 with disruptive mutation
mM	millimole
MMS	Methyl methanesulfonate
Mth	*Methanobacterium thermoautotrophicum*
NaCl	Sodium Chloride
nM	nanomole
NT	Amino terminal
ORC	Origin Recognition Complex
PAGE	Polyacrylamide Gel Electrophoresis
PCR	Polymerase Chain Reaction
PS1	Pre-sensor 1
Psf1	Partner of Sld five protein 1
Psf2	Partner of Sld five protein 2
Psf3	Partner of Sld five protein 3
S	(DNA) Synthesis Phase
S. cerevisiae	*Sacchromyces cerevisiae*
SDS-PAGE	Sodium Dodecyl Sulfate Polyacrylamide Gel Electrophoresis
SF3	Super Family 3
Sld5	Synthetic lethal with Dpb11-1 protein 5
ssDNA	single stranded Deoxyribonucleic Acid
Sso	*Sulfolobus solfataricus*

SV40   Simian Virus 40

Tris   Tris (Hydroxymethyl) Aminomethane

URA3   gene that encodes for orotidine 5'-phosphate decarboxylase

            (uracil biosynthesis enzyme)

UTR   Untranslated region

YPD   Yeast extract-Peptone-Dextrose

3'   3 prime end

5-FOA   5-fluoroorotic acid

5'   5 prime end

CHAPTER 1: INTRODUCTION

1.1   The cell cycle in eukaryotes.

The general mechanisms governing the eukaryotic cell cycle are well conserved from unicellular organisms such as the budding yeast, *Saccharomyces cerevisiae* (*S. cerevisiae*) to higher order organisms such as humans [1]. One of the key classes of proteins responsible for regulating the cell cycle is the cyclin dependent kinases (Cdk). There are three main classes of Cdks each responsible for transitioning a cell into different cell cycle phases namely, G1-to-S, G2-to-M, and M-to-G1 [1]. Cdks phosphorylate transcriptional repressors and activators to bring about transcriptional changes in cells necessary for cell cycle progression. The most well studied phase change is the G1 through S transition. The G1 to S phase transition is referred to as the restriction point and is tightly regulated because cells become committed to DNA replication and cell division after entering S phase. In budding yeast, the levels of the early G1 cyclin, Cln3 increase in response to cell growth. Binding of Cln3 to Cdk1 permits phosphorylation of a transcriptional repressor Whi5, which releases it from binding to the promoters of two late G1 cyclins Cln1 and Cln2. These two late G1 cyclins further inactivate Whi5 and also activate transcription factors responsible for transcribing S phase cyclins that promote progression to S phase for DNA replication. The combination of negative feedback on the repressor Whi5 and unrestrained synthesis of S phase cyclins commits the cell ultimately towards DNA replication and cell division.

1.2   Eukaryotic DNA replication overview.

DNA replication is a crucial biological process that ensures each divided cell contains a copy of their genome. This biological process is tightly regulated allowing DNA replication to occur only once during the S phase of the cell cycle. Furthermore, a multitude of proteins are recruited to origins of replication in a series of steps. This leads to the unwinding of the double stranded DNA to single stranded templates which allows DNA polymerases to begin replication. The first step in this multistep pathway requires that the replicative helicase referred to as minichromosome maintenance proteins 2-7 (Mcm2-7) be loaded onto origins of replication. This Mcm loading is aided by the origin recognition complex (ORC), cell division control 6 (Cdc6), and Cdc10-dependent transcript 1 (Cdt1). After loading Mcm2-7, the S – phase Cdks and Dbf4 dependent kinase (DDK) are required to phosphorylate Mcm2-7 and other targets. Subsequently, the assembly of a heterotetrameric protein complex consisting of Sld5, Psf1, Psf2, and Psf3 also known as GINS along with cell division control 45 (Cdc45) promotes the initiation of DNA unwinding, allowing replication to commensurate [2].

1.3   Recruitment of Mcm2-7 to origins of replication.

In *S. cerevisiae* replication origins are autonomous replicating sequences 100 – 150 bp long [3]. These DNA sequences are recognized by the origin recognition complex (ORC) that aids in the recruitment of the Mcm2-7 complex in eukaryotes. ORC is comprised of six different subunits, namely Orc1-6 [4, 5]. Collectively, they bind replication origins forming a crescent moon-shaped complex that bends the DNA; it is this structure which allows the loading of Mcm2-7 (Figure. 1) [6]. Cryo-EM structures

suggest that Mcm2-7 is loaded as a double hexamer in a N-terminal head to head fashion (Figure 2) [7, 8]. Current models suggest the loading process at origins is achieved in an ATP dependent manner whereby a trimer of Mcm3, 5, and 7 and a tetramer of 2, 4, 6, and Cdt1 are brought together at an ORC-Cdc6 complex [9]. Consistent with this view, nuclear import of the Mcm 3, 5, and 7 trimer and the Mcm2, 4, 6, and Cdt1 tetrameric complex is reliant on nuclear localization signals found only on Mcm3 and Mcm2 subunits to bring in their respective trimeric and tetrameric complexes into the nucleus. Upon proper loading of the Mcm2-7 complex at origins, ORC-Cdc6 ATPase activity is thought to promote the release of Cdt1 via conformational changes of the loaded complex. However, if all Mcm subunits including Cdt1 are not present at the origin or loaded in the correct conformation, the ATPase activity of ORC-Cdc6 will promote the release of all Mcm subunits allowing further loading attempts [9]. Additional studies of loading at origins of replication have revealed the time dependent manner in which double hexamers are established at the origin where the first hexamer forms rapidly, while the second one takes longer [10]. The N terminal head to head loading of double hexamers allows bidirectional replication fork progression. The loaded Mcm2-7 complex at origins is referred to as a pre-replication complex (pre-RC) and does not possess the ability to unwind DNA until additional events that will be discussed later on are completed [1].
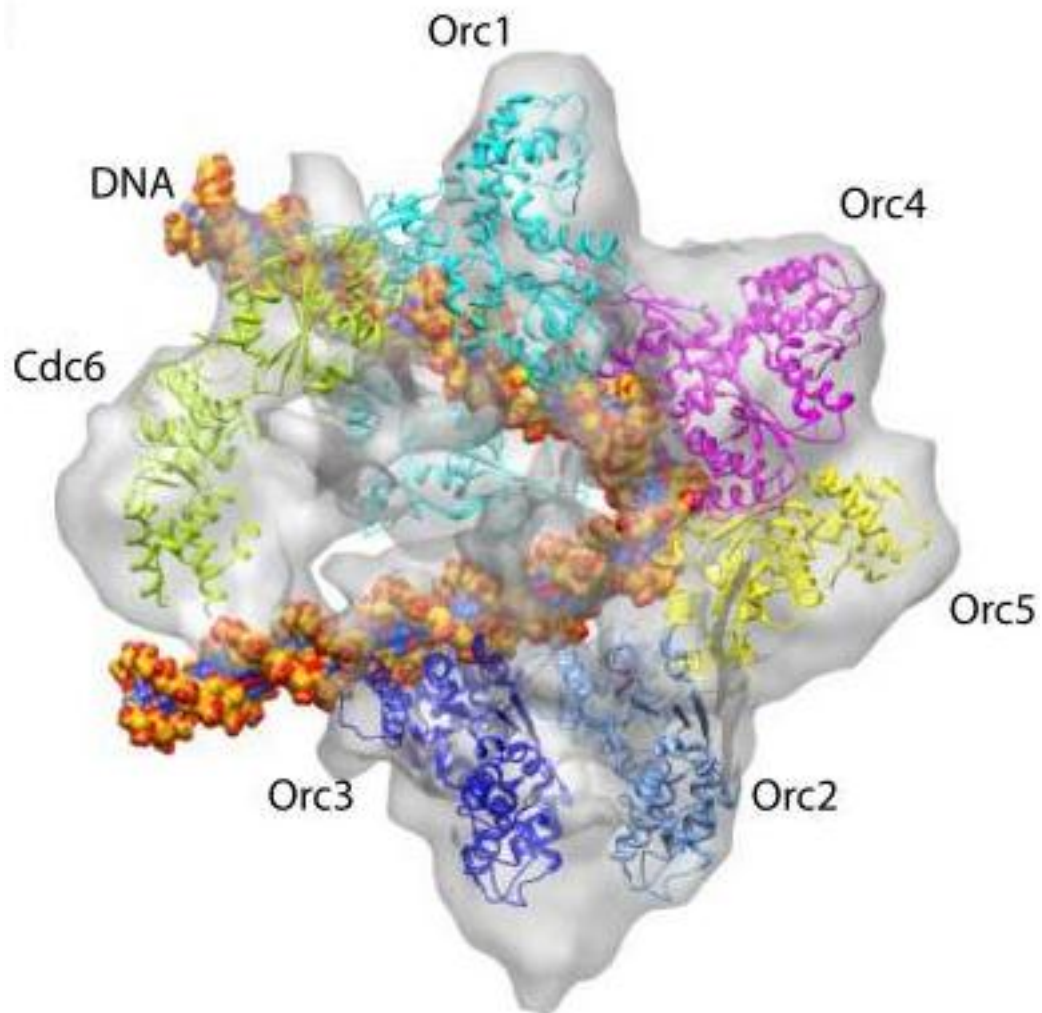
Figure 1. Model of ORC/Cdc6 complex bound to DNA. The Orc subunits 1-5 with

Cdc6 encircle DNA and is thought to bend the bound DNA. Orc6 a component of ORC,

is not shown for clarity which interacts with Orc2 and Orc3. Adapted from Sun *et al* [6].
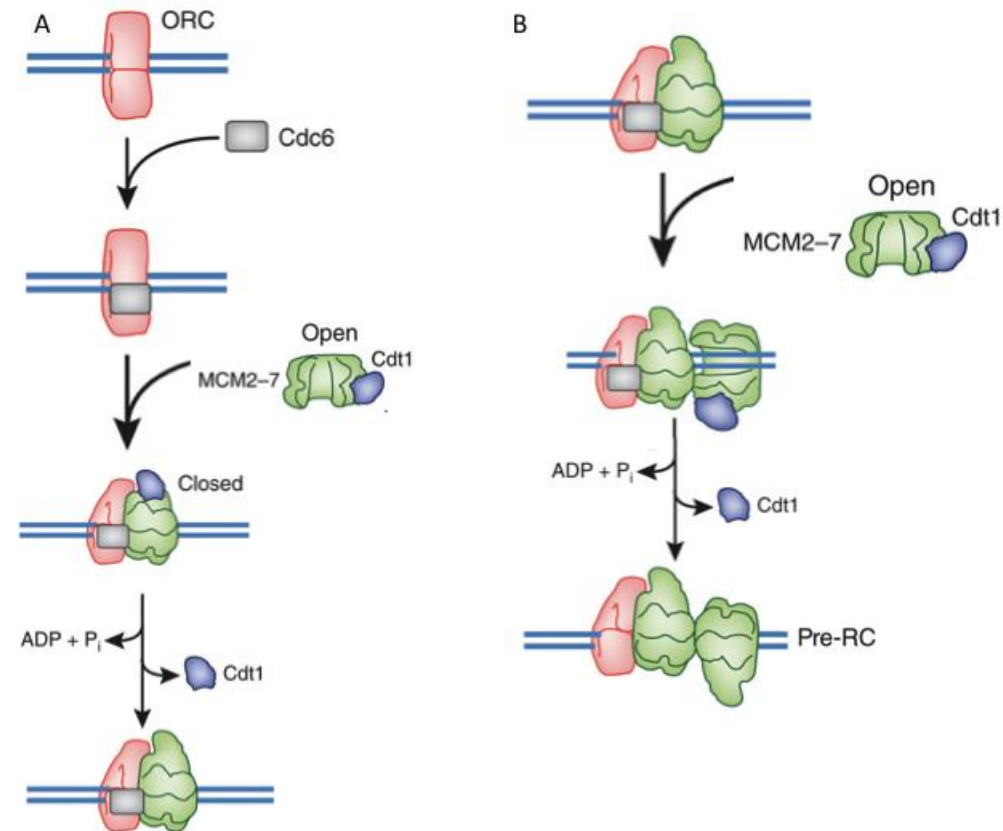
Figure 2. Model of Mcm2-7 loading onto ORC. (A) Initially, Cdc6 is recruited to ORC at DNA. Subsequently, the Mcm2-7 along with Cdt1 binding to ORC stimulates Cdc6/Orc ATPase which releases Cdt1. (B) The bound Mcm2-7 complex to ORC recruits a second Mcm2-7 complex forming a double hexamer in a N terminal, head to head fashion termed a pre-replicative complex (Pre-RC). The Cdt1 is released in a similar manner as described in (A).

1.4   Mechanisms to regulate pre-RC formation to prevent DNA replication.

Many mechanisms exist to prevent re-replication of the genome that may lead to chromosome instability. One such mechanism involves phosphorylation of Orc2 and Orc6 by S phase Cdks. Specifically, phosphorylation of Orc6 impedes it from contacting Cdt1, thus preventing Mcm2-7 loading when DNA replication has already begun [11]. The phosphorylation of Cdt1 also causes it to accumulate in the cytoplasm [12, 13]. Furthermore, Geminin, a protein found in metazoans adds another level of regulation by binding to Cdt1 to form a complex and shuttles Cdt1 out of the nucleus during S – phase thus preventing Mcm2-7 loading at origins [14]. After initiation of DNA replication, the N – terminus of Cdc6 is also recognized by Cdc4/34/53 which targets Cdc6 for proteolysis, thus preventing Mcm2-7 reloading at origins [15].

1.5   The eukaryotic replicative helicase, Mcm2-7.

Mcm2-7 was initially identified in two screens in *S. cerevisiae*: one screen identified mutations that resulted in missegregation of a plasmid (minichromosome) [16-18] and the other identified mutations that affected cell cycle progression [19]. Subsequent biochemical studies *in vitro* revealed that only a subcomplex consisting of Mcm 4,6, and 7 had helicase activity [20]. In fact, addition of either Mcm2 or Mcm3/5 to the subcomplex inhibited helicase activity. Thus, Mcm4, 6, and 7 were thought to be the catalytic subunits while Mcm2, 3, and 5 were thought to be regulatory subunits [21]. *In vivo*, all six subunits are essential for the initiation and progression of DNA replication [22]. As the catalytic core at replication forks, this ring-shaped helicase encircles DNA and utilizes ATP to translocate along the strands to separate them.

1.5   Phosphorylation of the Mcm2-7 by DDK.

DDK is a dimeric complex comprised of a regulatory subunit, Dumbbell former protein 4 (Dbf4) and a kinase subunit, cell division control 7 (Cdc7) protein [23]. Initially, Dbf4 was identified in *S. cerevisiae* where mutations of *DBF4* resulted in arrested cells with dumbbell morphology [24, 25]. While the Cdc7 kinase is ubiquitously expressed, Dbf4 expression is highly regulated which consequently controls DDK activity in a cell. Consistent with this view, Dbf4 expression in the cell is highest during late G1 to S phase, which is required for starting DNA replication, and diminished at the end of mitosis [23, 26]. During the G1/S transition, DDK is required to phosphorylate and relieve an inhibitory motif found on the N terminus of Mcm4 [27, 28]. In addition to phosphorylating Mcm4, DDK targeted phosphorylation of Mcm6 mediates Cdc45 recruitment to the Mcm2-7 complex [27, 29]. Subsequently, the addition of the GINS proteins to the Cdc45/Mcm2-7 complex completes an active helicase termed the pre-initiation complex [30].

1.6   ATP sites of hexameric helicases.

Mcm2-7 is an ATP dependent helicase, which belongs to **A**TPases **A**ssociated with diverse cellular **A**ctivities (AAA+) superfamily of proteins [31]. Like other hexameric helicase members, functional ATP sites are formed at the interface of adjacent subunits. One subunit acting in *cis* contributes the Walker A motif for binding ATP, Walker B and sensor 1 for binding water for ATP hydrolysis, while the other neighbouring subunit acting in *trans* contributes the arginine finger and sensor 2 to hydrolyze the gamma phosphate of ATP [30]. Collectively, these sites are encoded in a region termed the AAA+ domain found in all AAA+ proteins [31]. Intriguingly, of all AAA+ hexameric helicases, only the eukaryotic Mcm2-7 is a heterohexameric complex, all others are homohexamers. In keeping with the heterogeneity of Mcm2-7, not all ATP sites are found to hydrolyze ATP even though all the ATP sites are essential *in vivo*. In assays looking for the pair wise ATPase activity of Mcm subunits, Mcm3/7 contributed the majority of ATPase activity, while Mcm2/5 had no detectable activity [32, 33]. Based on pair wise ATPase activity studies, the arrangement of the Mcm subunits was established and a gate, which would allow loading of the complex at origins of replication, proposed at the Mcm2/5 interface [32, 34] (Figure 3). This gate has been observed in EM studies, and closes upon interactions with GINS and Cdc45 [35]. The closure of the gate completes the ring formation around either single stranded or double stranded DNA, which most likely permits the Mcm2-7 complex to begin unwinding DNA. The ring shape of hexameric helicases is important for enhancing the processivity of the helicase allowing helicases such as Mcm2-7 to separate thousands of base pairs before collapsing [30].
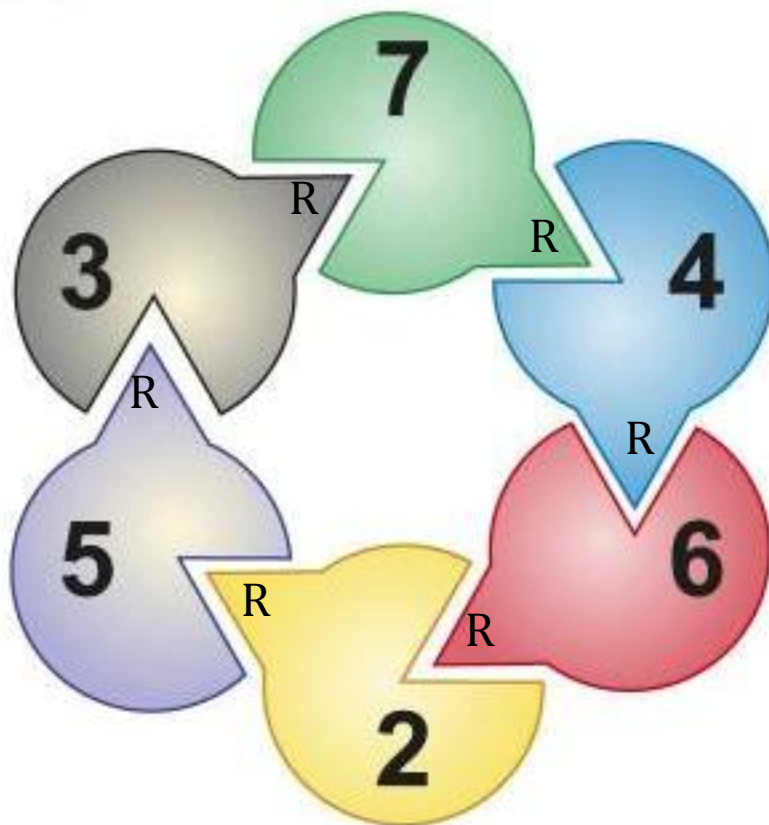
Figure 3. C-terminal view of the Mcm2-7 complex. The eukaryotic Mcm subunits are postulated to form the specific arrangement as shown above. The *trans* acting arginine finger (R) contributed by one subunit interacts with the ATP pocket of its neighbouring subunit to hydrolyze ATP (Adapted from Davey *et al*.) [32].

1.7   Structural overview of hexameric helicases.

Rapid developments have been made in crystallizing archaeal MCMs and related viral helicases providing structural insights into potential mechanisms of DNA unwinding [36]. Based on archaeal structures, such as the *Sulfolobus sofataricus* (Sso) MCM, a large N terminal domain and C terminal domain were identified that forms two globular heads on both ends of the helicase, connected by a slender waist (when viewed laterally) [36]. This general architecture was also confirmed for Mcm2-7 based on EM studies (Figure 4). A conserved region found between the N and C terminal domains referred to as the allosteric control loop facilitates communication between the N and C terminal domains during ATP binding and hydrolysis [37]. Four distinct β hairpins were identified in the near full length structure of Sso MCM. These β hairpins are protein structural motifs that are formed from two interacting strands of peptides oriented in an anti-parallel fashion. The Sso MCM β hairpins were named based on their location on the MCM subunit. The significance of these β hairpins will be discussed in more details later. The high sequence identity between different archaeal MCMs, related viral helicases, and Mcm2-7 suggests these structural features are most likely present in the eukaryotic Mcms.
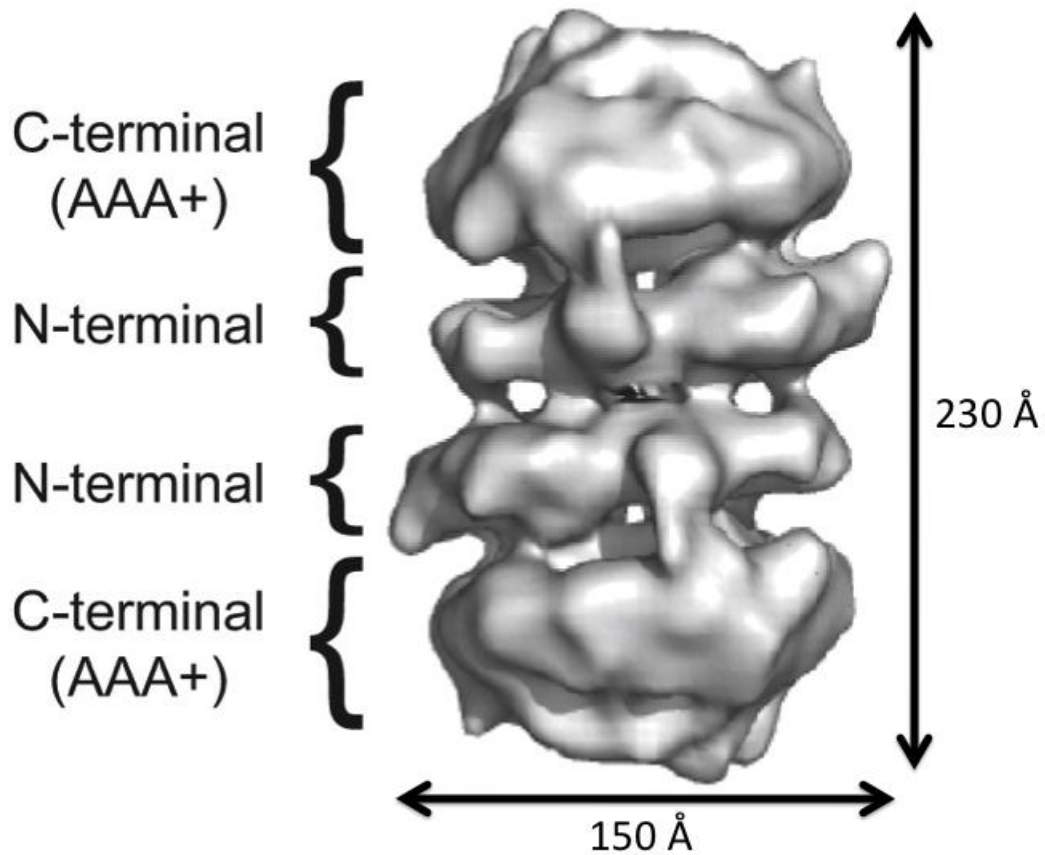
Figure 4. Electron micrograph of double Mcm2-7. The two Mcm2-7 complexes interact at the N terminal domains to form double hexamers at origins of replication during loading. The N and C terminal domains appear as globular domains with a thinner waist connecting the two domains as shown [7].

1.8   β Hairpins and their role in hexameric helicases.

As previously mentioned, four β hairpins were identified from the structure of SsoMCM, which are also conserved in eukaryotic Mcms. Biochemical studies of these β hairpins have revealed that these have important functions in the mechanism of DNA unwinding (Figure 5). The N – terminal (NT) β hairpin is the only β hairpin found in the N terminal domain. It is located within the central channel of the helicase, and mutation of basic amino acids on the tip of the NT β hairpin abrogates DNA unwinding *in vitro* [38]. Further mutational analysis of the NT β hairpin in eukaryotic Mcms suggests this β hairpin is required for initial binding of the Mcm2-7 during loading [39].

The pre-sensor (PS) 1 β hairpin, which is located on the N-terminal side of the sensor 1 region is involved in DNA translocation in both viral and archaeal helicases [38]. The sensor 1 region is responsible for detecting the ATP or ADP status of the binding pocket. Intriguingly the PS1 β hairpin is located within the central channel at the C terminal domain, however there are subtle differences in regards to the amount of protrusion into the central channel during β hairpin movement. In the SsoMCM, the PS1 β hairpin is more recessed to the wall of the central channel, whereas in the simian virus 40 helicase, the PS1 β hairpin protrudes further into the central channel [36].

The helix 2 insert (H2I) β hairpin is also found in the C terminal domain of the helicase. This β hairpin forms a short alpha helix at the tip of the β hairpin and is thought to be involved in separating the dsDNA as it enters the central channel, acting like a wedge. Based on fluorescence spectroscopy, the H2I β hairpin of the archaebacteria,

Methanobacterium thermoautotrophicum (Mth) MCM is predicted to move from a hydrophilic to hydrophobic environment during ATP binding and hydrolysis in the helicase subunits [40]. Deletion of this β hairpin in the Mth MCM results in loss of DNA unwinding *in vitro* [40].

The external (Ext) β hairpin is located on the outer surface and near a side channel according to structural studies of archaeal MCMs [41]. This side channel is thought to be an exit point for unwound DNA where the Ext β hairpin may direct ssDNA away. Mutation of the Ext β hairpin in Sso MCM disrupts DNA unwinding and demonstrates that this β hairpin is involved in DNA binding [42].
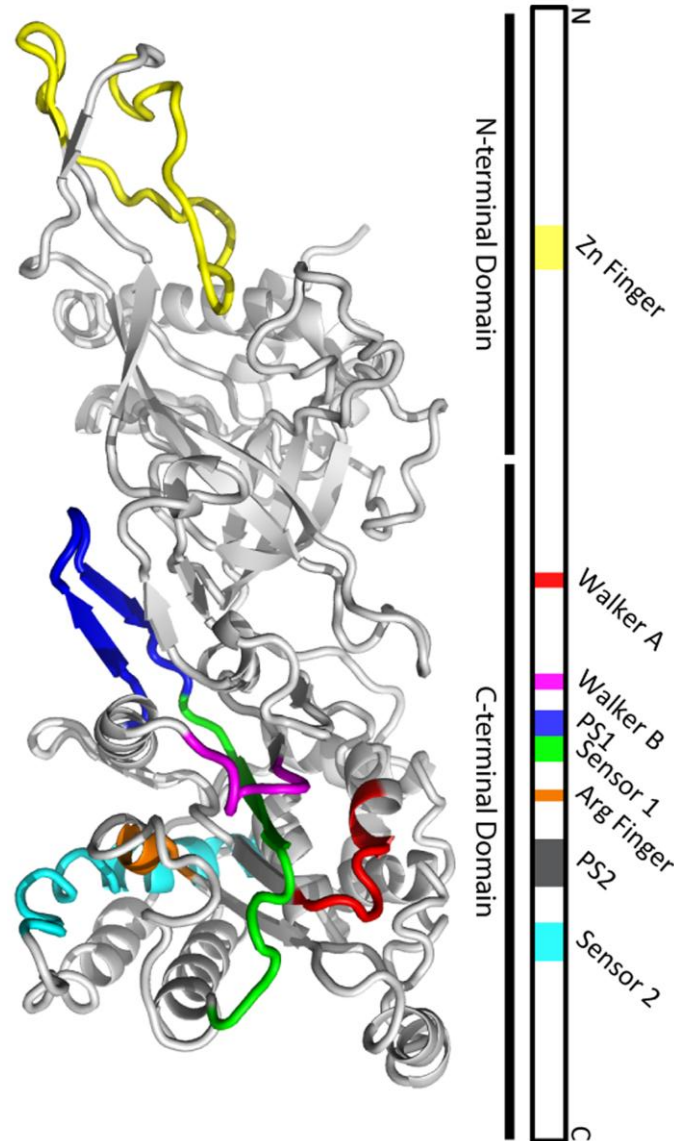
Figure 5. **Structure of the Mcm proteins.** Organization of the Mcm proteins in both the linear protein sequence (right) and in the folded proteins, based on the crystal structure of the *Solfolobus solfataricus* Mcm protein (PDB-ID 3F9V); [7]. The Mcm proteins are members of the AAA+ family of ATPases. The ATPase active sites are formed at the interface between two subunits. The Walker A (red), Walker B (magenta), and Sensor-1 (green) motifs are contributed by one subunit; the Arginine Finger (orange) and Sensor-2 (cyan) motifs are contributed by a second subunit (reviewed in 13). The Pre-Sensor 1 motif (PS1; blue) harbors a conserved lysyl residue at the turn between the two β-strands,

and is not directly involved in ATP hydrolysis; this lysyl residue is the subject of the current work. For clarity, the PS2 motif is not indicated on the 3-dimensional structure. The central channel would be located on the left side of the Mcm subunit, while the external face would be located on the right side of the Mcm subunit. From Lam *et al* [43].

1.9   Models for ATP hydrolysis and coordinated conformational changes in hexameric helicases.

In the bovine papillomavirus E1 (E1) helicase structure, each PS1 β hairpin forms a salt bridge with the phosphate backbone of DNA bound within the ring. Further analysis of the E1 structure shows that the PS1 β hairpins track along the DNA in a spiral staircase manner [44]. This suggested that DNA translocation occurs in a step wise manner where a single cycle of ATP binding, hydrolysis, and release moves a single nucleotide through the helicase [44]. Crystal structure data supports this view since each of the PS1 β hairpins is found at a different height within the ring and their positions depend on the helicase subunits' ATP, ADP, or apo status. The PS1 β hairpin is found at the top of the staircase in the ATP bound state, in an intermediate position in the ADP bound state, and at the bottom of the staircase in the apo state [44]. The information gathered from these structural studies provides a model where ATP hydrolysis sequentially moves DNA through the E1 helicase one nucleotide at a time.

The large tumour antigen of the simian virus (SV) 40 helicase, also an AAA+ hexameric helicase, utilizes a different ATP dependent mechanism to translocate and unwind DNA compared to the E1 helicase. In structural studies of the SV40 helicase, the nucleotide binding sites were either all bound to ATP, ADP, or none at all. This observation suggests a concerted model for ATP binding and hydrolysis to drive DNA unwinding. When ATP is bound to the helicase subunits, the central channel narrows, whereas in the apo state, the central channel is wider [45]. In this concerted model, the channel constricts like an iris during ATP binding and hydrolysis, and at the same time

the PS1 β hairpin makes a 17Å movement into the central channel to move DNA through [45].

The model for archaeal MCMs postulates ATP driven DNA unwinding acting in a semi-sequential manner. In biochemical studies where wild type ssoMCM subunits and mutant ssoMCM subunits containing Walker A mutations were mixed, helicase activity was observed when at least three wild type subunits were found in the complex. Furthermore, these wild type subunits had to be adjacent to one another in order to have helicase activity [46]. Together, these studies suggest that archaeal MCMs require only a subset of functional ATP sites to unwind DNA.

1.10   Models for DNA translocation and unwinding.

Three main models for how Mcm2-7 translocates and unwinds DNA have been proposed (Figure 6). These models are based mainly on experimental evidence collected from homohexameric helicases. Although Mcm2-7 is a heterogenous complex, structural features found in archaeal MCMS and related viral helicases would most likely be present in eukaryotic Mcms due to the high conservation of the protein sequences. This is especially true of the AAA+ domain containing C terminal domain of all Mcms and its related viral helicase subunits [30, 31, 36].

The steric exclusion model for DNA unwinding proposes that Mcm2-7 translocates along one strand and separates the other strand passively similar to DnaB in *E. coli* [47] (Figure 6B). Crystal structure of the E1 helicase bound to ssDNA suggests this would be the case. Each PS1 β hairpin located in the centre of the helicase makes an electrostatic interaction with the sugar phosphate backbone of ssDNA via a lysine residue. Through ATP binding and hydrolysis the β hairpin moves the ssDNA through the central channel one nucleotide at a time in a stair case manner [44]. Recent data suggests this is a likely method for eukaryotic replicative helicases. A streptavidin molecule located on the leading strand blocks DNA replication, while the same block on the lagging strand has no effect using S phase Xenopus egg extracts to load onto a DNA template [48].

The ploughshare model posits that a "wedge or pin" structure in the centre of the ring splits the DNA apart as it is threaded through the helicase ring (Figure 6C).

Subsequently, the separated strands exit either through the N terminal end of the helicase or through one of the side channels of the helicase. As previously mentioned, a helix 2 insert (H2I) β hairpin located in the central channel based on the Mth MCM is postulated to act as the wedge [40]. Deletion of the H2I β hairpin in the Mth MCM results in loss of helicase activity. Furthermore, fluorescence studies suggest the H2I β hairpin makes a significant conformational change during ATP binding and hydrolysis bringing the β hairpin from a hydrophobic to hydrophilic environment [40]. This same H2I β hairpin is also found in eukaryotic Mcms. The Davey lab began deleting the H2I β hairpin in budding yeast Mcms and determined deletion mutants did not support viability (unpublished).

The strand extrusion model is another possible mechanism utilized by Mcm2-7 to unwind DNA (Figure 6D). This model has dsDNA enter the central channel, one of the separated strands exit through a side channel, and the other single strand exiting through the N terminal end. Side channels large enough to accomodate ssDNA have been observed in cryo-EM structures of Mcm2-7 and crystal structures of archaeal MCMs [7, 41]. As previously discussed, mutational studies of each of the 4 β hairpins located in MCMs result in ATPase, DNA binding and unwinding defects, which provide insight into the importance of these β hairpin structures in hexameric helicases. This suggests that the strand extrusion model is attractive because it satisfies the evidence gathered whereby all β hairpins play a role in Mcm2-7 in DNA unwinding.
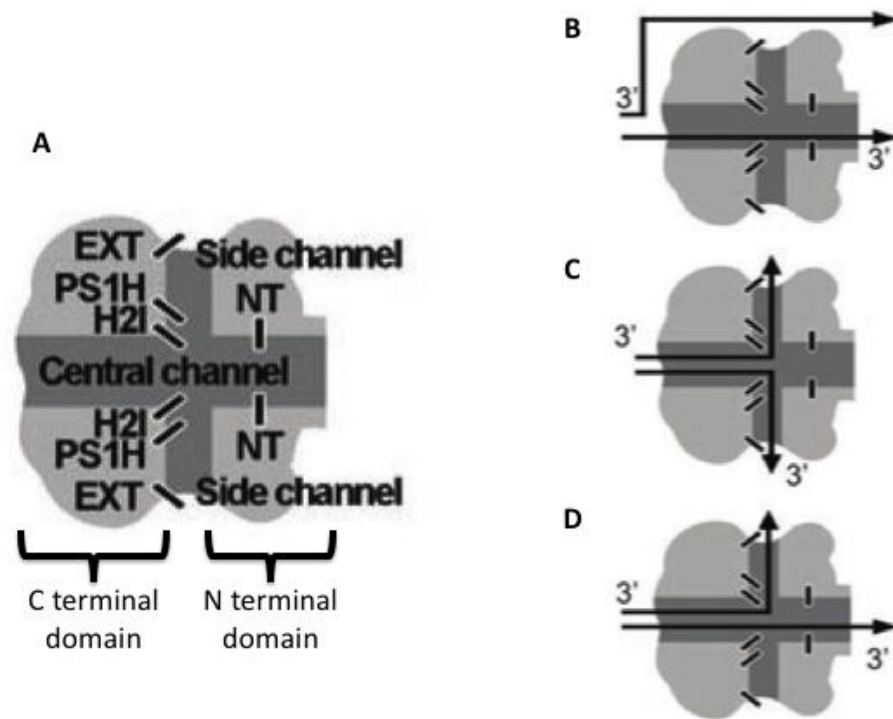
Figure 6. Models for DNA translocation in Mcm2-7. (A) The Mcm2-7 is sliced in half laterally though the central channel. The relative location of the 4 β hairpins, namely N terminal (NT) β hairpin, pre-sensor 1 (PS1) β hairpin, helix 2 insert (H2I) β hairpin, and external (EXT) β hairpin are shown in two of the six subunits in Mcm2-7. (B) In the steric exclusion model, the leading strand moves through the central channel while the lagging strand is passively unwound. (C) In the ploughshare model, both strands of DNA enters the channel and is split by the H2I β hairpin and exits through side channels. (D) The strand extrusion model postulates that both strands enter the central channel and one strand exits through the N terminal end while the other strand is extruded through the side channel. Adapted from Brewster and Chen [36].

1.11   Scope of thesis and hypothesis.

DNA replication is a crucial biological process. Aberrant DNA replication can lead to genomic instability, which is associated with human diseases such as cancer. During replicative stress the Mcm2-7 is a target of the DNA damage response to prevent further DNA unwinding in order to allow the cell to recover [49]. Despite its importance, the molecular mechanism of Mcm2-7 DNA translocation along DNA during DNA unwinding is unclear.

This thesis seeks to address the role of the PS1 β hairpin in eukaryotic Mcm2-7. I hypothesize that the PS1 β hairpin is involved in DNA translocation by facilitating the movement of DNA through the central channel of Mcm2-7 during DNA unwinding. To characterize the PS1 β hairpin *in vivo*, genetic mutations were introduced into budding yeast Mcms to determine viability. ATPase, helicase, and DNA binding were also measured *in vitro* to identify molecular defects associated with mutating the PS1 β hairpin. Together these experiments provide insight into the function of the PS1 β hairpin in regards to their contributions to the mechanism of DNA translocation and unwinding in Mcm2-7.

1.12   Chapter 1 References

1. Bertoli, C., Skotheim, J.M., and de Bruin, R.A. (2013) Control of cell cycle transcription during G1 and S phases. *Nat.Rev.Mol.Cell Biol.* **14,** 518-528
2. Bell, S.P., and Dutta, A. (2002) DNA replication in eukaryotic cells. *Annu.Rev.Biochem.* **71,** 333-374
3. Marahrens, Y., and Stillman, B. (1992) A yeast chromosomal origin of DNA replication defined by multiple functional elements. *Science.* **255,** 817-823
4. Bell, S.P., and Stillman, B. (1992) ATP-dependent recognition of eukaryotic origins of DNA replication by a multiprotein complex. *Nature.* **357,** 128-134
5. Bell, S.P., Mitchell, J., Leber, J., Kobayashi, R., and Stillman, B. (1995) The multidomain structure of Orc1p reveals similarity to regulators of DNA replication and transcriptional silencing. *Cell.* **83,** 563-568
6. Sun, J., Kawakami, H., Zech, J., Speck, C., Stillman, B., and Li, H. (2012) Cdc6-induced conformational changes in ORC bound to origin DNA revealed by cryo-electron microscopy. *Structure.* **20,** 534-544
7. Remus, D., Beuron, F., Tolun, G., Griffith, J.D., Morris, E.P., and Diffley, J.F. (2009) Concerted loading of Mcm2-7 double hexamers around DNA during DNA replication origin licensing. *Cell.* **139,** 719-730
8. Gambus, A., Khoudoli, G.A., Jones, R.C., and Blow, J.J. (2011) MCM2-7 form double hexamers at licensed origins in Xenopus egg extract. *J.Biol.Chem.* **286,** 11855-11864
9. Frigola, J., Remus, D., Mehanna, A., and Diffley, J.F. (2013) ATPase-dependent quality control of DNA replication origin licensing. *Nature.* **495,** 339-343
10. Fernandez-Cid, A., Riera, A., Tognetti, S., Herrera, M.C., Samel, S., Evrin, C., Winkler, C., Gardenal, E., Uhle, S., and Speck, C. (2013) An ORC/Cdc6/MCM2-7 complex is formed in a multistep reaction to serve as a platform for MCM double-hexamer assembly. *Mol.Cell.* **50,** 577-588
11. Nguyen, V.Q., Co, C., and Li, J.J. (2001) Cyclin-dependent kinases prevent DNA re-replication through multiple mechanisms. *Nature.* **411,** 1068-1073
12. Tanaka, S., and Diffley, J.F. (2002) Interdependent nuclear accumulation of budding yeast Cdt1 and Mcm2-7 during G1 phase. *Nat.Cell Biol.* **4,** 198-207
13. Nguyen, V.Q., Co, C., Irie, K., and Li, J.J. (2000) Clb/Cdc28 kinases promote nuclear export of the replication initiator proteins Mcm2-7. *Curr.Biol.* **10,** 195-205
14. Dahmann, C., Diffley, J.F., and Nasmyth, K.A. (1995) S-phase-promoting cyclin-dependent kinases prevent re-replication by inhibiting the transition of replication origins to a pre-replicative state. *Curr.Biol.* **5,** 1257-1269
15. Drury, L.S., Perkins, G., and Diffley, J.F. (1997) The Cdc4/34/53 pathway targets Cdc6p for proteolysis in budding yeast. *EMBO J.* **16,** 5966-5976
16. Maine, G.T., Sinha, P., and Tye, B.K. (1984) Mutants of *S. cerevisiae* defective in the maintenance of minichromosomes. *Genetics.* **106,** 365-385
17. Sinha, P., Chang, V., and Tye, B.K. (1986) A mutant that affects the function of autonomously replicating sequences in yeast. *J.Mol.Biol.* **192,** 805-814
18. Tye, B.K. (1999) Minichromosome maintenance as a genetic assay for defects in DNA replication. *Methods.* **18,** 329-334

19. Moir, D., and Botstein, D. (1982) Determination of the order of gene function in the yeast nuclear division pathway using cs and ts mutants. *Genetics.* **100,** 565-577

20. Ishimi, Y. (1997) A DNA helicase activity is associated with an MCM4, -6, and -7 protein complex. *J.Biol.Chem.* **272,** 24508-24513

21. Bochman, M.L., and Schwacha, A. (2007) Differences in the single-stranded DNA binding activities of MCM2-7 and MCM467: MCM2 and MCM5 define a slow ATP-dependent step. *J.Biol.Chem.* **282,** 33795-33804

22. Labib, K., Tercero, J.A., and Diffley, J.F. (2000) Uninterrupted MCM2-7 function required for DNA replication fork progression. *Science.* **288,** 1643-1647

23. Hughes, S., Elustondo, F., Di Fonzo, A., Leroux, F.G., Wong, A.C., Snijders, A.P., Matthews, S.J., and Cherepanov, P. (2012) Crystal structure of human CDC7 kinase in complex with its activator DBF4. *Nat.Struct.Mol.Biol.* **19,** 1101-1107

24. Johnston, L.H., and Thomas, A.P. (1982) A further two mutants defective in initiation of the S phase in the yeast *Saccharomyces cerevisiae. Mol.Gen.Genet.* **186,** 445-448

25. Johnston, L.H., and Thomas, A.P. (1982) The isolation of new DNA synthesis mutants in the yeast Saccharomyces cerevisiae. *Mol.Gen.Genet.* **186,** 439-444

26. Ferreira, M.F., Santocanale, C., Drury, L.S., and Diffley, J.F. (2000) Dbf4p, an essential S phase-promoting factor, is targeted for degradation by the anaphase-promoting complex. *Mol.Cell.Biol.* **20,** 242-248

27. Sheu, Y.J., and Stillman, B. (2006) Cdc7-Dbf4 phosphorylates MCM proteins via a docking site-mediated mechanism to promote S phase progression. *Mol.Cell.* **24,** 101-113

28. Sheu, Y.J., and Stillman, B. (2010) The Dbf4-Cdc7 kinase promotes S phase by alleviating an inhibitory activity in Mcm4. *Nature.* 463, 113-117

29. Randell, J.C., Fan, A., Chan, C., Francis, L.I., Heller, R.C., Galani, K., and Bell, S.P. (2010) Mec1 is one of multiple kinases that prime the Mcm2-7 helicase for phosphorylation by Cdc7. *Mol.Cell.* **40,** 353-363

30. Bochman, M.L., and Schwacha, A. (2009) The Mcm complex: unwinding the mechanism of a replicative helicase. *Microbiol.Mol.Biol.Rev.* **73,** 652-683

31. Duderstadt, K.E., and Berger, J.M. (2008) AAA+ ATPases in the initiation of DNA replication. *Crit.Rev.Biochem.Mol.Biol.* **43,** 163-187

32. Davey, M.J., Indiani, C., and O'Donnell, M. (2003) Reconstitution of the Mcm2-7p heterohexamer, subunit arrangement, and ATP site architecture. *J.Biol.Chem.* **278,** 4491-4499

33. Bochman, M.L., Bell, S.P., and Schwacha, A. (2008) Subunit organization of Mcm2-7 and the unequal role of active sites in ATP hydrolysis and viability. *Mol.Cell.Biol.* **28,** 5865-5873

34. Bochman, M.L., and Schwacha, A. (2010) The *Saccharomyces cerevisiae* Mcm6/2 and Mcm5/3 ATPase active sites contribute to the function of the putative Mcm2-7 'gate'. *Nucleic Acids Res.* **38,** 6078-6088

35. Costa, A., Ilves, I., Tamberg, N., Petojevic, T., Nogales, E., Botchan, M.R., and Berger, J.M. (2011) The structural basis for MCM2-7 helicase activation by GINS and Cdc45. *Nat.Struct.Mol.Biol.* **18,** 471-477

36. Brewster, A.S., and Chen, X.S. (2010) Insights into the MCM functional mechanism: lessons learned from the archaeal MCM complex. *Crit.Rev.Biochem.Mol.Biol.* **45,** 243-256

37. Barry, E.R., Lovett, J.E., Costa, A., Lea, S.M., and Bell, S.D. (2009) Intersubunit allosteric communication mediated by a conserved loop in the MCM helicase. *Proc.Natl.Acad.Sci.U.S.A.* **106,** 1051-1056

38. McGeoch, A.T., Trakselis, M.A., Laskey, R.A., and Bell, S.D. (2005) Organization of the archaeal MCM complex on DNA and implications for the helicase mechanism. *Nat.Struct.Mol.Biol.* **12,** 756-762

39. Leon, R.P., Tecklenburg, M., and Sclafani, R.A. (2008) Functional conservation of beta-hairpin DNA binding domains in the Mcm protein of *Methanobacterium thermoautotrophicum* and the Mcm5 protein of *Saccharomyces cerevisiae*. *Genetics.* **179,** 1757-1768

40. Jenkinson, E.R., and Chong, J.P. (2006) Minichromosome maintenance helicase activity is controlled by N- and C-terminal motifs and requires the ATPase domain helix-2 insert. *Proc.Natl.Acad.Sci.U.S.A.* **103,** 7613-7618

41. Brewster, A.S., Wang, G., Yu, X., Greenleaf, W.B., Carazo, J.M., Tjajadi, M., Klein, M.G., and Chen, X.S. (2008) Crystal structure of a near-full-length archaeal MCM: functional insights for an AAA+ hexameric helicase. *Proc.Natl.Acad.Sci.U.S.A.* **105,** 20191-20196

42. Brewster, A.S., Slaymaker, I.M., Afif, S.A., and Chen, X.S. (2010) Mutational analysis of an archaeal minichromosome maintenance protein exterior hairpin reveals critical residues for helicase activity and DNA binding. *BMC Mol.Biol.* **11,** 62-2199-11-62

43. Lam, S.K.W., Ma, X., Shilton, B.H., Sing, T.L., Brandl, C.J., and Davey, M.J. (2013) The PS1 hairpin of Mcm3 is essential for viability and for DNA unwinding *in vitro*. *PlosOne*.

44. Enemark, E.J., and Joshua-Tor, L. (2006) Mechanism of DNA translocation in a replicative hexameric helicase. *Nature.* **442,** 270-275

45. Gai, D., Zhao, R., Li, D., Finkielstein, C.V., and Chen, X.S. (2004) Mechanisms of conformational change for a replicative hexameric helicase of SV40 large tumor antigen. *Cell.* **119,** 47-60

46. Moreau, M.J., McGeoch, A.T., Lowe, A.R., Itzhaki, L.S., and Bell, S.D. (2007) ATPase site architecture and helicase mechanism of an archaeal MCM. *Mol.Cell.* **28,** 304-314

47. Itsathitphaisarn, O., Wing, R.A., Eliason, W.K., Wang, J., and Steitz, T.A. (2012) The hexameric helicase DnaB adopts a nonplanar conformation during translocation. *Cell.* **151,** 267-277

48. Fu, Y.V., Yardimci, H., Long, D.T., Ho, T.V., Guainazzi, A., Bermudez, V.P., Hurwitz, J., van Oijen, A., Scharer, O.D., and Walter, J.C. (2011) Selective bypass of a lagging strand roadblock by the eukaryotic replicative DNA helicase. *Cell.* **146,** 931-941

49. Charych DH, Coyne M, Yabannavar A, Narberes J, Chow S, et al. (2008) Inhibition of Cdc7/Dbf4 kinase activity affects specific phosphorylation sites on MCM2 in cancer cells. J Cell Biochem 104: 1075−1086.

CHAPTER 2: THE PS1 β HAIRPIN OF MCM3 IS ESSENTIAL FOR VIABILITY AND FOR DNA UNWINDING *IN VITRO*.

The contents in this chapter arise with modifications from Lam *et al* .

<u>Simon K.W. Lam</u>, Xiaoli Ma, Tina L. Sing, Brian H. Shilton, Christopher J. Brandl, and Megan J. Davey. The PS1 hairpin of Mcm3 is essential for viability and for DNA unwinding *in vitro*. (2013) PlosOne.

2.1   Introduction

In order for DNA replication to occur, the DNA duplex strands need to be separated by a replicative helicase [1]. Cellular replicative helicases tend to be hexameric rings that bind DNA within their central channels [2,3]. The ring shape is thought to maintain association with DNA thus enhancing the processivity of the helicase [4], and may be important for DNA unwinding by potentially excluding one strand from the central channel [5,6]. Regardless of the exact mechanism for DNA unwinding, the helicase must use nucleotide binding and hydrolysis to translocate along the bound DNA.

X-ray structures of homo-hexameric replicative helicases that are members of the AAA+ family, including the superfamily 3 (SF3) helicase from bovine papillomavirus (E1) and minichromosome maintenance (MCM) from archaeal species, provide insight into how DNA translocation is achieved [7−10]. Notably, a β hairpin from each subunit projects into the central channel of the helicase. The structure of the E1 hexameric helicase with single- stranded DNA in its central channel identifies residues at the tip of the β hairpin that contact the sugar phosphate backbone; in particular a lysine side-chain forms a salt-bridge with the DNA backbone [11]. ATP binding and hydrolysis are thought to drive

conformational changes, leading to a sweeping motion of the b hairpins that moves DNA through the central channel [9]. Later structures of archaeal MCM proteins demonstrated the existence of the b hairpins with a lysine residue near the tip [7,10]. These hairpins are referred to as the pre-sensor 1 (PS1) β hairpins due to their position adjacent to the sensor 1 motif of the AAA+ domain as shown for the *Sulfolobus solfataricus* (Sso) MCM (Figure 1). Mutation of the conserved lysine in archaeal MCM proteins abrogates its helicase activity, but only slightly affects DNA binding, consistent with a role in DNA translocation [12].

In eukaryotic cells, the replicative helicase is comprised of six paralogous proteins of the AAA+ family, termed Mcm2-7. Each of the six subunits is essential for DNA replication in cells from yeast to mammals [13,14]. The requirement for six distinct subunits may reflect the greater need for control of DNA replication and hence cell proliferation in eukaryotic cells compared to other systems. Indeed, the Mcm2-7 subunits are differentially targeted by protein kinases for control of cell proliferation [15–25], and have distinct roles in the activity of the intact complex [26]. In this regard, ATP sites found within each of the Mcm subunits are formed at the interface of neighboring subunits, and contribute differently to the overall ATPase activity of the complex [26–28]. Not all of the ATP sites are essential for DNA unwinding, even though the ATP sites are essential for viability [28–31]. Models for DNA unwinding by the homo-hexameric helicases suggest each subunit makes an identical contribution. This is not the case for Mcm2-7 as suggested by the distinct sequences of the components and the different ATPase activity of subunit pairs [26,27]. However, the exact contribution each subunit

makes to the DNA unwinding by Mcm2-7 is currently unknown.

Here, we have mutated the conserved lysine residue in the PS1 β hairpin of each of the *Saccharomyces cerevisiae* Mcm2-7 subunits to alanine and examined the effect of the mutations. Interestingly, only the PS1 β hairpin of Mcm3 is essential for viability. Mutation of the PS1 hairpin in Mcm7 resulted in growth related phenotypes, and strains with pairwise mutations in the remaining PS1 hairpins displayed synthetic slow or lethal interactions. Consistent with the observed loss of viability, Mcm2-7 complexes containing Mcm3 bearing the PS1 mutation ($Mcm3_{K499A}$) show decreased DNA unwinding in vitro. The $Mcm3_{K499A}$-containing Mcm2-7 has reduced binding to single-stranded DNA in an electrophoretic mobility shift assay, and analysis of $Mcm3_{K499A}$ in yeast cell extracts revealed differences in its molecular associations. Together our results indicate the importance of the PS1 β hairpins in Mcm2-7 function, and identify an essential function of Mcm3.
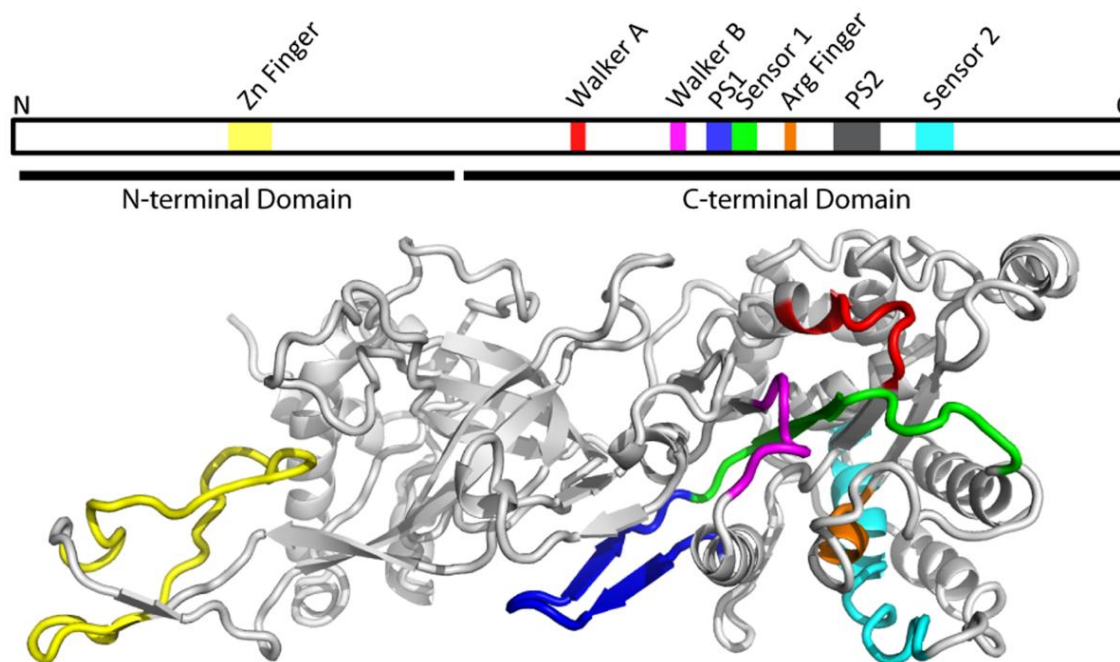
Figure 1. **Structure of the Mcm proteins.**

Organization of the Mcm proteins in both the linear protein sequence (top) and in the folded proteins, based on the crystal structure of the *Solfolobus solfataricus* Mcm protein (PDB-ID 3F9V); [7]. The Mcm proteins are members of the AAA+ family of ATPases. The ATPase active sites are formed at the interface between two subunits. The Walker A (red), Walker B (magenta), and Sensor-1 (green) motifs are contributed by one subunit; the Arginine Finger (orange) and Sensor-2 (cyan) motifs are contributed by a second subunit (reviewed in 13). The Pre-Sensor 1 motif (PS1; blue) harbors a conserved lysyl residue at the turn between the two β-strands, and is not directly involved in ATP hydrolysis; this lysyl residue is the subject of the current work. For clarity, the PS2 motif is not indicated on the 3-dimensional structure. doi:10.1371/journal.pone.0082177.g001

2.2   Materials and Methods

2.2.1 Plasmids

Oligonucleotides used to construct plasmids are listed in Table 1. For plasmid shuffling of the MCM genes, two plasmids for each wild-type gene were constructed (plasmids are listed in Table 2). The first set (pMD264, 245, 244, 227 238 and 228, representing MCM2 through 7, respectively) in the URA3-containing centro- meric plasmid YCplac33 [32] were amplified by PCR using a UTR primer and coding primer, and contained the promoter region and coding sequence for each MCM. Oligonucleotide pairs MD81/MD82, MD83/MD84, MD85/MD86, MD87/MD88, MD89/MD90, and MD90/MD91 were used to amplify *MCM2*, *MCM3*, *MCM4*, *MCM5*, *MCM6*, and *MCM7*, respectively. The amplified *MCM* was then ligated into YCplac33 using the restriction enzyme cut sites indicated with the primers in Table 1. The second set of wildtype genes were cloned in YCplac111 (*LEU2-CEN*; [32]). For *MCM3* through *MCM6* these were constructed in a two-step process. The promoter region was amplified by PCR using a UTR primer and a start primer, then inserted into YCplac111 using the restriction sites in Table 1 (pMD229, 230, 232 and 240). A *Blp*I linker was then inserted into the polylinker *Sma*I site of the vector for *MCM4* and *MCM5* (pMD242 and 237). The remaining coding region was then inserted from a pET expression plasmids [27] using *Nde*I-*Sac*I for *MCM3* (pMD235), *Nde*I-*Blp*I for *MCM4* and *MCM5* (pMD379 and 378), and *Nde*I-*Bam*HI for *MCM6* (pMD239). For *MCM7*, the promoter region plus coding sequence up to the *Sal*I site at 251 base pairs was amplified by PCR using oligonucleotides (MD91 and 113) and cloned into YCplac111 (pMD241). pMD241 was digested with *Sma*I and a

*Blp*I linker inserted to generate pMD260. The remaining coding sequence of *MCM7* was inserted from a pET expression plasmid [27] using *Sal*I and *Blp*I to give pMD261. To generate $mcm3_{K499A}$- (pMD386; MD432/MD433), $mcm4_{K658A}$- (pMD391; MD411/MD412), $mcm5_{K506A}$- (pMD411; MD434/ 435), $mcm6_{K665A}$- (pMD358; MD413/MD414), $mcm3_{K499R}$- (MD501; MD612/MD613), $mcm3_{K499Q}$- (pMD558; MD661/ MD662), and $mcm3_{K499N}$- (pMD559; MD663/MD664) YC- plac111, the Stratagene QuikChange site-directed mutagenesis kit was used with the indicated primer pairs. Isolated clones were sequenced.

To clone *MCM3* (pMD562) and $mcm3_{K499A}$ (pMD563) into YEplac181, a *Sph*I-*Sac*I fragment of pMD235 and pMD386 was ligated into the same sites of YEplac181. A fragment of *Sph*I-*Sac*I from pMD386 was also ligated to the same sites in YIplac211 to generate $mcm3_{K499A}$-YIplac211 (pMD561). For cloning $mcm4_{K658A}$ into YIplac211, we first amplified $mcm4_{K658A}$ by PCR using oligonucleotides MD85, MD274, and mcm4$_{K658A}$-YCplac111 as template. This product was cloned into YIplac211 using *Pst*I and *Bam*HI to give pMD438. For $mcm5_{K506A}$, a *Blp*I site was introduced into YIplac211 at the *Sma*I site. $mcm5_{K506A}$ was introduced into this plasmid from $mcm5_{K506A}$-YCplac111 as a *Sph*I-*Blp*I fragment (pMD439). pMD440 was constructed by inserting a *Sph*I-*Bam*HI fragment of $mcm6_{K665A}$-YCplac111 into YIplac211. To generate *MCM3* and $mcm3_{K499A}$ myc[9] N-terminally tagged expression plasmids, *MCM3* and $mcm3_{K499A}$ were amplified by PCR using oligonucleotides MD84, MD556, and cloned using *Not*I and *Sac*I into a derivative of YCplac111 where the *DED1* promoter drives expression of a *myc*[9] N-terminally tagged protein [33]. The pET24a-$mcm3_{K499A}$ was cloned by cutting $mcm3_{K499A}$-

YCplac111 with *Nde*I and *Sac*I and ligating into the same sites of pET24a.

To construct MCM3 and mcm3$_{K499A}$ Flag[3]-tagged expression plasmids, a *GAL10*

promoter containing YCplac111 plasmid (pMD407) was linearized with *Nde*I and *Sac*I.

Oligonucleotides MD659/MD660 were annealed and ligated into linearized pMD407.

MCM3 and *mcm3$_{K499A}$* isolated from pMD502 and pMD503 were then inserted as *Not*I-

*Sac*I fragments to give pMD560 and pMD554.

#	Description	Site	Sequence (5'-3')
MD81	MCM2 UTR	SphI	TTGGTCGCATGCACTTTTCATCTAAATGGATTA
MD82	MCM2 coding	SacI	TAGTGTGAGCTCTTATCCAGATATTCGTAGGAA
MD83	MCM3 UTR	SphI	AAGGTCGCATGCGTTATTTTTCTCTTTTTTTTCAA
MD84	MCM3 coding	SacI	TAGTGTGAGCTCAGTAAACATTCCTGTGACAT
MD85	MCM4 UTR	PstI	TTAGCTCTGCAGACTTGAACGGATCTTTAGTAT
MD86	MCM4 coding	SacI	TAGTGTGAGCTCGGAATGATTGTAGTAGACAG
MD87	MCM5 UTR	SphI	TTGGTCGCATGCTTTGTAAAAACAAAGAGTAAAATT
MD88	MCM5 coding	SmaI	TATTATCCCGGGAAGGCGTCAAGCTAAGAC
MD89	MCM6 UTR	PstI	TTAGCTCTGCAGTTGAAAAAAACCAGTTTTAACC
MD90	MCM6 coding	BamHI	TATTATGGATCCATCCGCAAGAGTGCACTG
MD91	MCM7 UTR	SphI	TTGGTCGCATGCAAGGAAAGGCCGTTTTT
MD92	MCM7 coding	SmaI	TATTATCCCGGGAAAGAATGAAGGCCCTGT
MD109	MCM3 start	SalI	TTAGTCGTCGACATATGTAATTGACGTTTGTATCTTTT
MD110	MCM4 start	SacI	TTAGTCGAGCTCATATGTTTTAAGTTCTTGAGGTTC
MD111	MCM5 start	SmaI	TTAGTCCCGGGCATATGTTATCTGGCTTCTAATTCAC
MD134	MCM6 start	XbaI	ATAATCTAGACATATGAAAAAAACCAGTTTTAACCT
MD113	MCM7	SalI	ATTATAGTCGACAGGAAGC
MD274	MCM4 coding	BglII	TGATTGTAGAGATCTTCAGACACGGTTATTCAG
MD411	MCM4$_{K658A}$ coding	MspA1I	GCAGACTATTTCAATCGCAGCAGCGGGAATTATCACAACAC
MD412	MCM4$_{K658A}$ noncoding	MspA1I	GTGTTGTGATAATTCCCGCTGCTGCGATTGAAATAGTCTGC
MD413	MCM6$_{K665A}$ coding	PstI	CAGACCATCTCTATTGCTGCAGCTGGTATTCACGCTAC
MD414	MCM6$_{K665A}$ noncoding	PstI	GTAGCGTGAATACCAGCTgcAGCAATAGAGATGGTCTG
MD434	MCM5$_{K506A}$ coding	AlwNI	ACAATCTCCATCGCAGCAGCTGGTATCACTACAGTGC
MD435	MCM5$_{K506A}$ noncoding	AlwNI	GCACTGTAGTGATACCAGCTGCTGCGATGGAGATTGT
MD432	MCM3$_{K499A}$ coding	SacII	CAAACGGTGACGATTGCCGCGGCAGGTATTCACACAAC
MD433	MCM3$_{K499A}$ noncoding	SacII	GTTGTGTGAATACCTGCCGCGGCAATCGTCACCGTTTG
MD556	MCM3 coding	NotI	ATGACGCGGCCGCCATGGAAGGCTCAACGGGATT
MD612	MCM3$_{K499R}$ coding		AAACGGTGACGATTGCCCGGGCAGGTATTCACACAACA
MD613	MCM3$_{K499R}$ noncoding		TGTTGTGTGAATACCTGCCCGGGCAATCGTCACCGTTT
MD661	MCM3$_{K499Q}$ coding		ACAAACGGTGACGATTGCCCAAGCAGGTATTCACACAA
MD662	MCM3$_{K499Q}$ noncoding		TTGTGTGAATACCTGCTTGGGCAATCGTCACCG TTTGT
MD663	MCM3$_{K499N}$ coding		AAACGGTGACGATTGCCAATGCAGGTATTCACACAACA
MD664	MCM3$_{K499N}$ noncoding		TGTTGTGTGAATACCTGCATTGGCAATCGTCACCGTTT
MD659	Flag[3] coding	NdeI NotI overhangs	TATGGATTATAAAGATGATGATGATAAAGCTGCTGATTATAAAGATGATGATGATAAAG CTGCTGATTATAAAGATGATGATGATAAAGC
MD660	Flag[3] noncoding	NdeI NotI overhangs	GGCCGCTTTATCATCATCATCTTTATAATCAGCAGCTTTATCATCATCAT CTTTATAATCAGCAGCTTTATCATCATCATCTTTATAATCCA

Table 1. Oligonucleotides used in this study.

Plasmid	Description
pMD264 [30]	*MCM2*-YCplac33
pMD245	*MCM3*-YCplac33
pMD244	*MCM4*-YCplac33
pMD227	*MCM5*-YCplac33
pMD238	*MCM6*-YCplac33
pMD228	*MCM7*-YCplac33
pMD229	*MCM3* 5′UTR-YCplac111
pMD230	*MCM4* 5′UTR-YCplac111
pMD232	*MCM5* 5′UTR-YCplac111
pMD240	*MCM6* 5′UTR-YCplac111
pMD241	*MCM7* 5′UTR-YCplac111
pMD266	*MCM2*-YCplac33-pLU9
pMD235	*MCM3*-YCplac111
pMD242	*MCM4* 5′UTR-YCplac111 (*Blp*I)
pMD379	*MCM4* YCplac111
pMD237	*MCM5* 5′UTR-YCplac111 (*Blp*I)
pMD378	*MCM5*-YCplac111
pMD239	*MCM6*-YCplac111
pMD260	*MCM7* 5′UTR-YCplac111 (*Blp*I)
pMD261	*MCM7*-YCplac111
pMD307	$mcm2_{K633A}$-YCplac111
pMD386	$mcm3_{K499A}$-YCplac111
pMD391	$mcm4_{K658A}$-YCplac111
pMD411	$mcm5_{K506A}$-YCplac111
pMD358	$mcm6_{K665A}$-YCplac111
pMD308	$mcm7_{K550A}$-YCplac111
pMD438	$mcm4_{K658A}$-YIplac211
pMD439	$mcm5_{K506A}$-YIplac211
pMD440	$mcm6_{K665A}$-YIplac211
pMD346	$mcm7_{K550A}$-YIplac211
pMD466	$mcm3_{K499A}$-pET24a
pMD501	$mcm3_{K499R}$-YCplac111
pMD558	$mcm3_{K499Q}$-YCplac111
pMD559	$mcm3_{K499N}$-YCplac111
pMD502	*DED1-myc^9-MCM3*-YCplac111
pMD503	*DED1-myc^9-mcm3$_{K499A}$*-YCplac111
pMD407	*GAL10*-YCplac111
pMD554	*GAL10-Flag^3-mcm3$_{K499A}$*-YCplac111
pMD560	*GAL10-Flag^3-MCM3*-YCplac111
pMD561	$mcm3_{K499A}$-YIplac211
pMD562	*MCM3*-YEplac181
pMD563	$mcm3_{K499A}$-YEplac181

Table 2. **Plasmids used in this study.**

2.2.2 Plasmid shuffling

Diploid heterozygous strains containing a *KanMX* deletion of a *mcm* gene were obtained from Open Biosystems. The *mcm2*::*his3* disruption strain (MDY54) was a derivative of YMD33 [31]. Each of these was transformed with the relevant *MCM*-YCplac33 plasmid and sporulated to give MDY16, 17, 40, 41, 70, and 100. mcm deletion haploid strains containing their corresponding *MCM*- YCplac33 were transformed with a *mcmKA*-YCplac111 or *MCM*- YCplac111. The transformed strains were grown in YPD, then plated on 5-FOA-containing media to select for cells that lost the *MCM*-YCplac33 [34].

2.2.3 Yeast strains

All yeast strains are listed in Table 3. Two-step gene replacement was used to integrate PS1 hairpin mutation into the yeast genome [35]: $mcm2_{K633A}$ (MDY225 and 226), *MCM3*/*mcm3K499A* (MDY411), *mcm4K658A* (MDY220), $mcm5_{K506A}$ (MDY221 and 222), $mcm6_{K665A}$ (MDY258 and 259), $mcm7_{K550A}$ (MDY253 and 254). Each mutation incorporated a unique restriction site (Table 1) for identification. YIplac211 plasmids were linearized with *Msc*I (*mcm3*), *Age*I, (*mcm4*) *Bsp*EI (*mcm5*), *Msc*I (*mcm6*), or *Bam*HI (*mcm7*) and transformed into BY4743. URA3 positive colonies were grown in YPD liquid media, and then selected on 5-FOA-containing media. PCR amplification of the *MCM* loci was performed and restriction mapping used to confirm integration of mcm_{KA}. The heterozygous diploid strains were sporulated and haploid mcm_{KA} mutants isolated.

Yeast strain	Genotype
MDY16	MAT**a** his3Δ1 leu2Δ0 met15Δ0 ura3Δ0 mcm3Δ::KanMX (YCplac33 MCM3 URA3)
MDY17	MATa his3Δ1 leu2Δ0 met15Δ0 ura3Δ0 mcm4Δ::KanMX (YCplac33 MCM4 URA3)
MDY40	MATa his3Δ1 leu2Δ0 met15Δ0 ura3Δ0 mcm7Δ::KanMX (YCplac33 MCM7 URA3)
MDY41	MATa his3Δ1 leu2Δ0 met15Δ0 ura3Δ0 mcm6Δ::KanMX (YCplac33 MCM6 URA3)
MDY54	MATα leu2Δ0 MET15 ura2Δ0 lys2Δ0 mcm2::his3 (YCplac33 MCM2 URA3)
MDY70	MATa his3Δ1 leu2Δ0 met15Δ0 ura3Δ0 mcm2Δ::his3 (YCplac111 MCM2 LEU2)
MDY71	MAT**a** his3Δ1 leu2Δ0 met15Δ0 ura3Δ0 mcm2Δ::his3 (YCplac111 mcm2$_{K633A}$ LEU2)
MDY72	MATa his3Δ1 leu2Δ0 met15Δ0 ura3Δ0 mcm7Δ::KanMX (YCplac111 MCM7 LEU2)
MDY73	MAT**a** his3Δ1 leu2Δ0 met15Δ0 ura3Δ0 mcm7Δ::KanMX (YCplac111 mcm7$_{K550A}$ LEU2)
MDY100	MATa his3Δ1 leu2Δ0 met15Δ0 ura3Δ0 mcm5Δ::KanMX (YCplac33 MCM5 URA3)
MDY153	MATa his3Δ1 leu2Δ0 met15Δ0 ura3Δ0 mcm3Δ::KanMX (YCplac111 MCM3 LEU2)
MDY154	MATa his3Δ1 leu2Δ0 met15Δ0 ura3Δ0 mcm4Δ::KanMX (YCplac111 MCM4 LEU2)
MDY155	MAT**a** his3Δ1 leu2Δ0 met15Δ0 ura3Δ0 mcm4Δ::KanMX (YCplac111 mcm4$_{K658A}$ LEU2)
MDY172	MATa his3Δ1 leu2Δ0 met15Δ0 ura3Δ0 mcm5Δ::KanMX (YCplac111 MCM5 LEU2)
MDY173	MAT**a** his3Δ1 leu2Δ0 met15Δ0 ura3Δ0 mcm5Δ::KanMX (YCplac111 mcm5$_{K506A}$ LEU2)
MDY220	MAT**a** his3Δ1 leu2Δ0 ura3Δ0 mcm4$_{K658A}$
MDY221	MATα his3Δ1 leu2Δ0 ura3Δ0 mcm5$_{K506A}$
MDY222	MAT**a** his3Δ1 leu2Δ0 ura3Δ0 mcm5$_{K506A}$
MDY225	MATα his3Δ1 leu2Δ0 ura3Δ0 mcm2$_{K633A}$
MDY228	MATα his3Δ1 leu2Δ0 ura3Δ0 mcm4$_{K658A}$ mcm5$_{K506A}$
MDY229	MAT**a** his3Δ1 leu2Δ0 ura3Δ0 mcm4$_{K658A}$ mcm5$_{K506A}$
MDY253	MATα his3Δ1 leu2Δ0 ura3Δ0 mcm7$_{K550A}$
MDY254	MAT**a** his3Δ1 leu2Δ0 ura3Δ0 mcm7$_{K550A}$
MDY258	MATα his3Δ1 leu2Δ0 ura3Δ0 mcm6$_{K665A}$
MDY259	MAT**a** his3Δ1 leu2Δ0 ura3Δ0 mcm6$_{K665A}$
MDY402	MAT**a** his3Δ1 leu2Δ0 met15Δ0 ura3Δ0 mcm3Δ::KanMX (YCplac111 mcm3$_{K499R}$ LEU2)
MDY403	MAT**a** his3Δ1 leu2Δ0 met15Δ0 ura3Δ0 mcm6Δ::KanMX (YCplac111 MCM6 LEU2)
MDY404	MAT**a** his3Δ1 leu2Δ0 met15Δ0 ura3Δ0 mcm6Δ::KanMX (YCplac111 mcm6$_{K663A}$ LEU2)
MDY405	MAT**a** his3Δ1 leu2Δ0 met15Δ0 ura3Δ (YCplac111 DED1-myc^9-MCM3)
MDY406	MAT**a** his3Δ1 leu2Δ0 met15Δ0 ura3Δ (YCplac111 DED1-myc^9-mcm3$_{K499A}$)
MDY407	MAT**a** his3Δ1 leu2Δ0 met15Δ0 ura3Δ (YCplac111 GAL10-Flag^3-MCM3 LEU2)
MDY408	MAT**a** his3Δ1 leu2Δ0 met15Δ0 ura3Δ (YCplac111 GAL10-Flag^3-mcm3$_{K499A}$ LEU2)
MDY411	MAT**a**/α his3Δ1/his3Δ1 leu2Δ0/leu2Δ0 lys2Δ0/LYS2 met15Δ0/MET15 ura3Δ0/ura3Δ0 MCM3/mcm3$_{K499A}$
MDY414	MAT**a** his3Δ1 leu2Δ0 met15Δ0 ura3Δ0 mcm3Δ::KanMX (YEplac181 MCM3 LEU2)
BY4741 [52]	MAT**a** his3Δ1 leu2Δ0 met15Δ0 ura3Δ
BY4743 [52]	MAT**a**/α his3Δ1/his3Δ1 leu2Δ0/leu2Δ0 lys2Δ0 met15Δ0 ura3Δ0/ura3Δ0

Table 3. **Yeast strains used in this study.**

2.2.4 Imaging yeast overexpressing of *MCM3* and *mcm3$_{K499A}$*

BY4741 transformed with YCplac111-*GAL10-MCM3* or YC- plac111-*GAL10-mcm3$_{K499A}$* was grown in minimal media lacking leucine supplemented with 2% galactose overnight. The overnight cultures were diluted to 10^6 cells/mL with minimal media lacking leucine supplemented with 2% galactose. After two hours cells were imaged under bright field using a Nikon Eclipse Ti microscope. Measurements were taken using NIS Elements Imaging Software.

2.2.5 Proteins

The recombinant Mcm subunits were purified from *Escherichia coli* and reconstituted into Mcm2-7 as described [27].

2.2.6 Mcm3$_{K499A}$ purification

The mcm3$_{K499A}$ pET24a plasmid was transformed into BL21 DE3 Codon+. Twelve liters of transformed cells were grown in LB media with 100 mg/L of ampicillin, and 25 mg/L of chloramphenicol to a density of A600 = 0.6. Cells were cooled to 15°C and isopropyl β-D-1-thiogalactopyranoside added to a final concentration of 1 mM. Cells were incubated at 15°C for 20 hours prior to collecting the cell pellet. The cell pellet was resuspended in 250 mL of Buffer H (20 mM HEPES, pH 7.5, 2 mM DTT, 10% v/v glycerol, and 0.1 mM EDTA) and lysed at 15000 psi in an Emulsiflex-C3 high pressure homogenizer. Debris was pelleted by centrifugation at 15000 g for 25 minutes and the supernatant decanted. Ammonium sulfate was added to the supernatant (0.25 g/mL) with stirring at 4°C. Ammonium sulfate precipitate was collected by centrifugation, and

resuspended with 150 mL of Buffer H. The solution was dialyzed overnight at 4°C in 4 L

of Buffer H with stirring and then loaded onto a Fast flow Q Sepharose column

equilibrated with Buffer H and washed with 7 column volumes of Buffer H containing

50mM NaCl. Mcm3$_{K499A}$ was eluted over 10 column volumes in a gradient of 0–500 mM

NaCl in Buffer H. Fractions containing Mcm3$_{K499A}$ were collected and dialyzed overnight

in 750 mL of Buffer H at 4°C. A single-stranded (ss) DNA-Sepharose column was made

by coupling boiled and sonicated salmon sperm DNA to cyanogen bromide-activated

Sepharose 4B (GE Life Sciences). The dialyzed solution was loaded onto the ssDNA-

Sepharose column equilibrated with Buffer H, washed with 10 column volumes and

protein eluted with 10 column volumes of a 0–500 mM NaCl gradient in Buffer H. The

fractions containing Mcm3$_{K499A}$ were pooled and ammonium sulfate added (0.3 g/mL)

with stirring at 4μC. The precipitate was collected by centrifugation, resuspended and

dialyzed against 400 mL of Buffer A (20 mM Tris-HCl, pH 7.5, 2 mM DTT, 10% v/v

glycerol, and 0.1 mM EDTA). The solution was loaded onto a MonoQ (GE Life

Sciences) column equilibrated with Buffer A containing 50 mM NaCl, and the protein

eluted over 20 column volumes of a 0–500 mM NaCl gradient in Buffer A. Fractions

containing Mcm3$_{K499A}$ were pooled and dialyzed in one liter of Buffer H with stirring,

overnight at 4μC. The dialyzed solution was loaded onto a MonoS (GE Life Sciences)

column equilibrated with Buffer H containing 50 mM NaCl, and the protein eluted over

20 column volumes of a 0–500 mM NaCl gradient in Buffer H. Fractions were collected

and frozen at -80°C.

2.2.7 Western blotting

Western blotting was performed using polyvinylidene difluoride membranes and anti-myc (Sigma-Aldrich) as described by Mutiu *et al* [36].

2.2.8 Biochemical assays

DNA unwinding and ATPase assays were performed essentially as described by Stead *et al* [25] with the exception that intact complex was used. ATP hydrolysis was assayed using thin-layer chromatography. Each 15-ml reaction contained 1 mM [γ^{32}P] ATP (20 mCi/mmole; Perkin Elmer Life Sciences), 20 mM Tris–HCl (pH 7.5), 10 mM magnesium acetate, and 2 mM DTT, and 200 nM Mcm2-7. At the indicated times, 2 mL of each reaction was removed and quenched with 2 mL of 50 mM EDTA (pH 8). One microliter was spotted onto a polyethyleneimine cellulose sheet (EM Science), developed in 0.6 M potassium phosphate (pH 3.4), dried, exposed to a PhosphorStorage screen, and scanned with a Storm 860 scanner (GE Healthcare). DNA unwinding measurements were performed with a DNA substrate containing 30 nucleotides of duplex, with 60 nucleotides of single-stranded DNA on one strand and a 59 biotin on the other strand. Each reaction (6 mL) contained 20 mM Tris–HCl (pH 7.5), 10 mM magnesium acetate, 100 mM EDTA, 5 mM DTT, 5 mM ATP, 67 nM streptavidin, 1 nM substrate with 100 nM, 200 nM or 400 nM Mcm2-7. Samples were analyzed by native PAGE using an 8% gel in Tris–borate–EDTA buffer.

2.2.9 DNA binding assay

The single-stranded DNA affinity chromatography was per- formed with a 200 mL

single-stranded DNA Sepharose column (see above Mcm3$_{K499A}$ purification). Five

micrograms of Mcm2-7 complex were applied to the column in buffer H containing 5

mM ATP and 50 mM NaCl and eluted with buffer containing 5 mM ATP and either 50

mM, 100 mM, 200 mM, 300 mM, 400 mM, or 500 mM NaCl. Each elution was

performed twice with one column volume. 24 mL of each fraction was separated by SDS-

PAGE (6%). The polyacrylamide gels were stained with colloidal blue stain, and then

washed with deionized water to destain the gels for imaging. The destained gels were

then silver stained according to protocol provided in Pierce Silver Stain Kit (Thermo

Scientific) to detect protein in the column fractions.

The electrophoretic mobility shift assay was adapted from Stead *et al* [25]. Briefly,

Mcm2-7 and Mcm2-7$_{3K499A}$ complexes were incubated with 1nM of 59-end 32P-labeled

oligonucleotide (ATGTCCTAGCAAGCCAGAATTCGGCAGCGTC-(T)60) at 37uC in

buffer containing 20 mM Tris–HCl (pH 7.5), 10 mM magnesium acetate, 100 mM

EDTA, 5 mM DTT, and 5 mM ATP for 10 minutes. One microgram of anti-Mcm7

antibody (Santa Cruz Biotech) was added to another set of Mcm2-7 samples prior to

incubation with radiolabeled oligonucleotide to disrupt Mcm2-7 binding. Four microliters

of 12.5% glycerol was added to each reaction and then resolved in a 5% native (Tris–

borate– EDTA) polyacrylamide gel (19:1 acrylamide:bis–acrylamide; Bio-Shop Canada)

containing 5% glycerol, 0.1% NP-40 and 10 mM Mg(CH3COO)2 at 30 mA for 2.5

hours. The gel was dried, and exposed to film.

2.2.10   Gel filtration chromatography

Proteins extracts were prepared cryogenically as described by Saleh *et al* [37]. Five

mg of yeast extract prepared in 50 mM sodium phosphate pH 7.0, 150 mM NaCl was

loaded at a flow rate of 0.3 mL/min. onto a 24 mL FPLC Superose 6HR10/30 column

(Amersham Pharmacia Biotech.). Protein from 10 mL aliquots of 250 mL fractions for

wild type protein and 10 mL for Mcm3$_{K449A}$ were resolved by SDS-PAGE and proteins

detected by western blotting.

2.2.11   Modeling of *S. cerevisiae* Mcm2-7

Individual Mcm2 through Mcm7 subunits were modeled based on the 4.35Å

resolution structure of *Solfolobus solfataricus* Mcm (SsoMcm; PDB ID 3F9V; [7]). This

was done using a multiple sequence alignment incorporating SsoMcm residues 9 to 603

and residues 204 to 849 of Mcm2; 22 to 744 of Mcm3; 188 to 837 of Mcm4; 25 to 692 of

Mcm5; 109 to 839 of Mcm6; and 15 to 728 of Mcm7. The comparative modeling

protocol of Rosetta was used to thread the sequences onto the SsoMcm structure, build

loop regions and additional domains in the Mcm2 through Mcm7 subunits that were not

present in SsoMcm, and refine the overall structure of the subunits [38,39]. A model for

the Mcm2-7 hexamer was then assembled by superimposing the N-terminal domains of

the Mcm2 through Mcm7 subunits on the N-terminal domains of the *Methanobacterium*

thermoautotrophicum hexamer (PDB ID 1LTL; [40]). Molecular graphics were generated

using PyMOL (Version 1.5.0.5, Schrodinger, LLC) and electrostatic surface calculations

were carried out using PDB2PQR [41] and APBS [42].

2.3   Results and Discussion

2.3.1 Effects of PS1 mutations in Mcm2-7 on yeast growth

Each of the Mcm subunits contains a pre-sensor 1 (PS1) β hairpin adjacent to the

sensor 1 motif of the AAA+ domain (Figure 1). To determine whether the PS1 hairpin

motifs are important for the function of Mcm2-7, the replicative helicase in eukaryotic

cells, we mutated the conserved lysine residue to alanine in each of the Mcm subunits

(Figure 2A). The mutant genes, encoded on *LEU2-* containing centromeric plasmids,

were shuffled into haploid strains bearing a deletion in the corresponding mcm and

maintained by *MCM* on a *URA3*-containing centromeric plasmid. Lack of function of the

mutant Mcm subunit is indicated by the absence of growth on media containing 5-

fluoroorotic acid (5-FOA), which is toxic to *URA3*-expressing strains. Of the six

subunits, only a mutation in the Mcm3 PS1 β hairpin ($mcm3_{K499A}$) resulted in a loss of

viability on 5-FOA (Figure 2B). Slow growth was noted for the $mcm7_{K550A}$ strain, but it is

viable. To more fully compare the relative phenotypes of the $mcm3_{K499A}$ and $mcm7_{K550A}$

strains, we have also incubated the strains for an extended period (Figure S1). The

presence of the mutant allele as the sole copy of the mcm_{KA} in the viable strains was

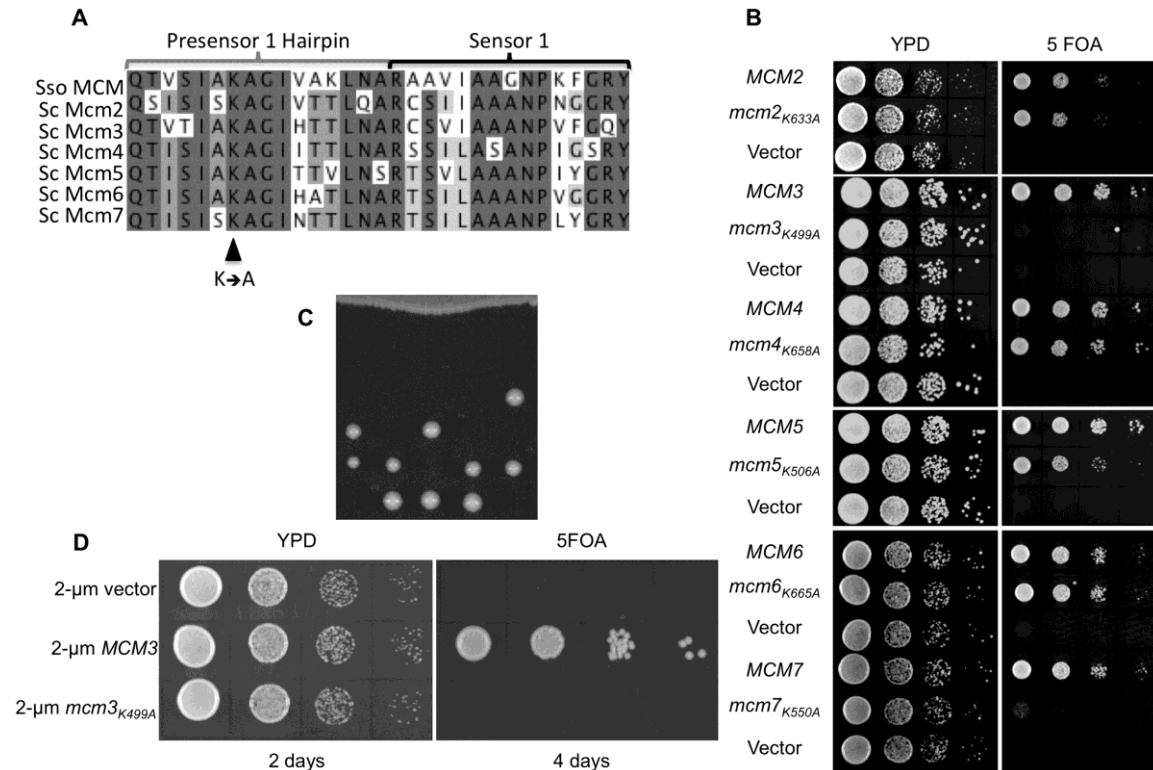confirmed by PCR and restriction digestion.

Figure 2. Growth of strains bearing the PS1 β hairpin alleles.

(A) Alignment of the PS1 β hairpin and Sensor 1 in SsoMcm with *S*. cerevisiae Mcm2-7

using T-Coffee. (B) Plasmid shuffling of Mcm PS1 β hairpin mutations. The wild-type

Mcm gene (*MCM*), the Mcm gene with PS1 β hairpin mutation (*mcm_{KA}*), or the empty

LEU2-CEN plasmid (Vector) were transformed into a haploid yeast strain deleted for the

genomic copy of the corresponding Mcm gene and containing a copy of the gene on a

URA3-CEN plasmid. Transformed yeast were grown overnight at 30°C in YPD media,

serially diluted, and then spotted onto a YPD plate or a plate containing 5-FOA. (C) The

diploid strain MDY411 (*MCM3/mcm3_{K499A}*) was sporulated and tetrads dissected. The

dissection plates (YPD) were incubated at 30°C. (D) MDY16 (*mcm3Δ::KanMX*

YCplac33 *MCM3 URA3*) was transformed with 2 micron plasmid YEplac181 (2-μm

Vector), pMD562 (2-μm *MCM3*), or pMD563 (2-μm *mcm3_{K499A}*). Transformants were

grown overnight at 30°C in YPD media, serially diluted, and then spotted onto a YPD

plate or a plate containing 5-FOA. doi:10.1371/journal.pone.0082177.g002

The Mcm genes were first identified through their requirement for the maintenance of autonomously replicating chromosomes in yeast [43]. To ensure that the inviability of the $mcm3_{K499A}$ strain was not due to a failure to maintain the plasmid, we integrated the $mcm3_{K499A}$ mutation into the diploid yeast strain BY4743 and analyzed the viability of spore colonies after sporulation and tetrad dissection. As shown in Figure 2C viability segregates in a 2:2 manner consistent with the inability of mcm3$_{K499A}$ to support growth. We also addressed whether $mcm3_{K499A}$ would support growth when overexpressed on a 2-micron plasmid by plasmid shuffling (Figure 2D). Similar to what we observed with the centromeric plasmid, no growth was detected. Further suggesting that the inability of $mcm3_{K499A}$ to support viability is not the result of reduced stability of the protein, we find that myc[9]-tagged wild- type Mcm3 and Mcm3$_{K499A}$ are found at a similar level (Figure S2). Taken together we conclude that the Mcm3 PS1 β hairpin is essential for the function of the Mcm2-7 complex.

To further characterize the effects of the PS1 mutations, we examined the growth of viable strains bearing the mutations at different temperatures (Figure 3A). For these experiments the PS1 β hairpin mutations were integrated into the genome. At each of the temperatures, the relative growth $mcm7_{K550A}$ was reduced. The $mcm2_{K633A}$ containing strain grew somewhat more slowly at 16°C. Mutations in the Mcm subunits often result in sensitivity to genotoxic agents. Therefore, we examined the growth of each of the strains with a PS1 mutation on media containing the ribonucleotide reductase inhibitor hydroxyurea, or the DNA-damaging agent methyl methanesulfonate (MMS) (Figure 3B). Consistent with its slow growth at different temperatures, strains containing $mcm7_{K550A}$

grew slowly on both agents, with a slight sensitivity to MMS noted. Similarly strains

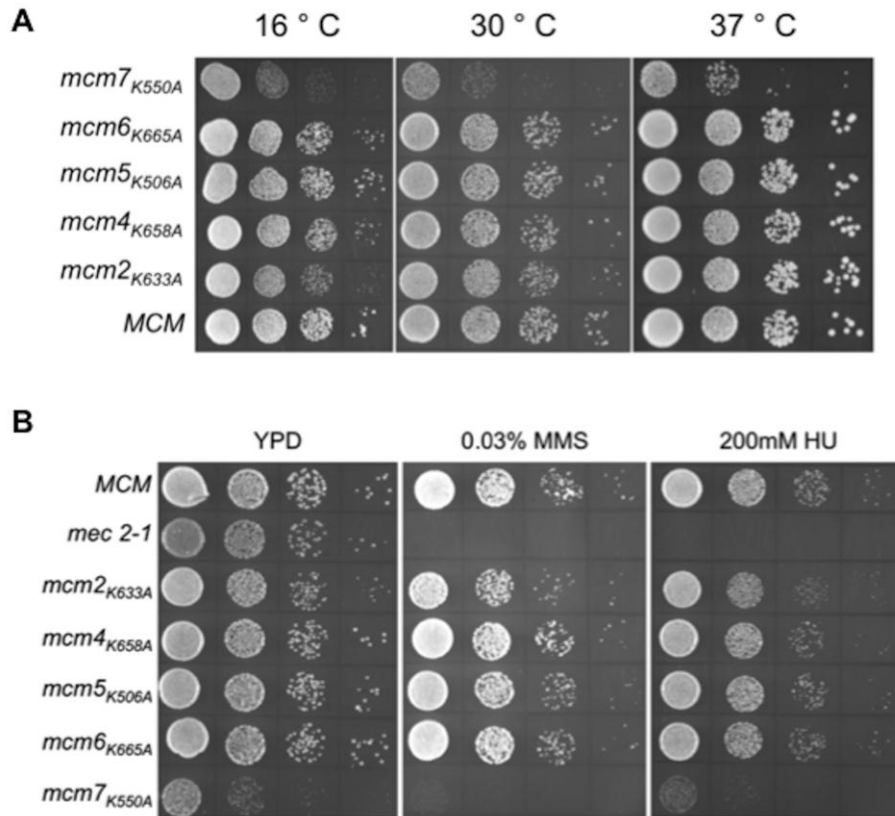bearing the other PS1 mutations were not sensitive to hydroxyurea or MMS.

Figure 3. Effect of temperature and genotoxic agents on PS1 β hairpin mutants.

(A) Cultures of yeast strains BY4741 (wild-type), MDY225 ($mcm2_{K633A}$), MDY220 ($mcm4_{K658A}$), MDY222 ($mcm5_{K506A}$), MDY256 ($mcm6_{K665A}$), and MDY254 ($mcm7_{K550A}$) were grown overnight in YPD at 30°C, serially diluted 10-fold, spotted onto YPD plates and incubated at either 16°C, 30°C or 37°C. (B) Cultures of yeast strains BY4741 (wild-type), MDY225 ($mcm2_{K633A}$), MDY220 ($mcm4_{K658A}$), MDY222 ($mcm5_{K506A}$), MDY256 ($mcm6_{K665A}$), and MDY254 ($mcm7_{K550A}$) were grown in YPD, and 10-fold serial dilutions spotted onto YPD and YPD containing either 0.03% methyl methanesulfonate (MMS) or 200 mM hydroxyurea (HU). Plates were incubated at 30°C. A mec2-1 [51] strain, known to be sensitive to genotoxic stress, was also spotted on the plates.

doi:10.1371/journal.pone.0082177.g003

Our plasmid shuffling experiments indicate that a single mutation of the conserved PS1 lysine (K499) residue in Mcm3 results in loss of viability. In contrast, the homo-hexameric *S. solfataricus* Mcm (SsoMcm) accommodates several subunits with disruptions in catalytic elements and still maintains significant helicase activity [44]. Therefore, we investigated the effect of mutating two different PS1 β hairpins in the Mcm2-7 complex. We mated the haploid strains containing individual PS1 β hairpin mutations to produce all the possible pair-wise combinations. After sporulating the heterozygous strains, we screened the spore colonies for viable double mutants. Only spore colonies with $mcm4_{K658A}$ and $mcm5_{K506A}$ were viable (Table 4). These grew more slowly than wild-type or strains containing either $mcm4_{K658A}$ or $mcm5_{K506A}$ and were more sensitive to hydroxyurea and MMS (Figure 4).
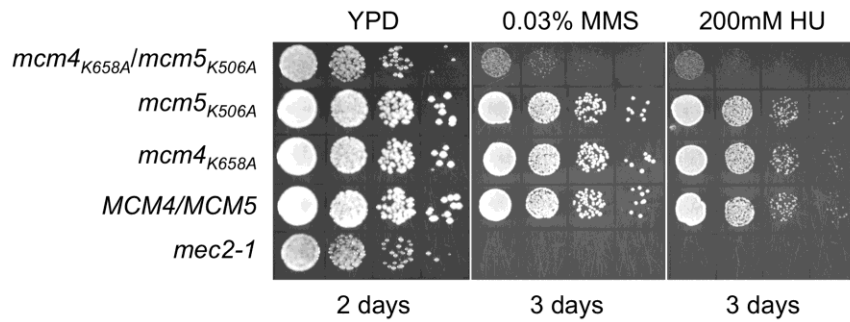
Figure 4. Phenotype of the *mcm4$_{K658A}$/mcm5$_{K506A}$* double mutant strain.

Haploid yeast strains containing either PS1 mutations in both Mcm4 and Mcm5 (MDY229), single PS1 mutations in either Mcm4 (MDY220) or Mcm5 (MDY222), and the wild-type strain BY4741 were grown overnight at 30°C in liquid YPD, serially diluted 10-fold, and then spotted onto YPD, YPD containing 0.03% methyl methanesulfonate (MMS), or 200 mM hydroxyurea (HU). A *mec2-1* [51] strain, known to be sensitive to genotoxic stress, was also spotted on the plates.

doi:10.1371/journal.pone.0082177.g004

Cross	Spore colonies examined[1]	Viable with two mutations	P - value
$mcm2_{K633A}$ x $mcm4_{K658A}$	24	0	0.002
$mcm2_{K633A}$ x $mcm5_{K506A}$	21	0	0.007
$mcm2_{K633A}$ x $mcm6_{K665A}$	18	0	0.007
$mcm2_{K633A}$ x $mcm7_{K550A}$	19	0	0.007
$mcm4_{K658A}$ x $mcm5_{K506A}$	24	6	0.161
$mcm4_{K658A}$ x $mcm6_{K665A}$	16	0	0.018
$mcm4_{K658A}$ x $mcm7_{K550A}$	15	0	0.018
$mcm5_{K506A}$ x $mcm6_{K665A}$	19	0	0.007
$mcm5_{K506A}$ x $mcm7_{K550A}$	21	0	0.007
$mcm6_{K665A}$ x $mcm7_{K550A}$	24	0	0.002

[1]A random spore analysis was performed by isolating individual spore colonies from tetrads.
doi:10.1371/journal.pone.0082177.t004

Table 4. Synthetic lethal crosses of *mcm* PS1 alleles.

The lysine residue on the PS1 β hairpin is predicted to make an electrostatic interaction with the sugar phosphate backbone of DNA to facilitate translocation of DNA and unwinding [8]. We converted the lysine of the PS1 β hairpin of Mcm3 to arginine, glutamine, or asparagine to determine whether the charge is important for function. Of the three alleles examined by plasmid shuffling, only $mcm3_{K499R}$ supported viability (Figure 5A). The strain containing this allele displayed no overt growth defects when plated on 200 mM hydroxyurea, 0.03% MMS, and 20 mM caffeine (Figure 5B). Additionally, the rate of growth was the same as wild type at 16°C, 30°C and 37°C (Figure 5C). This suggests that the positive charge at residue 499 of Mcm3 is essential for function.
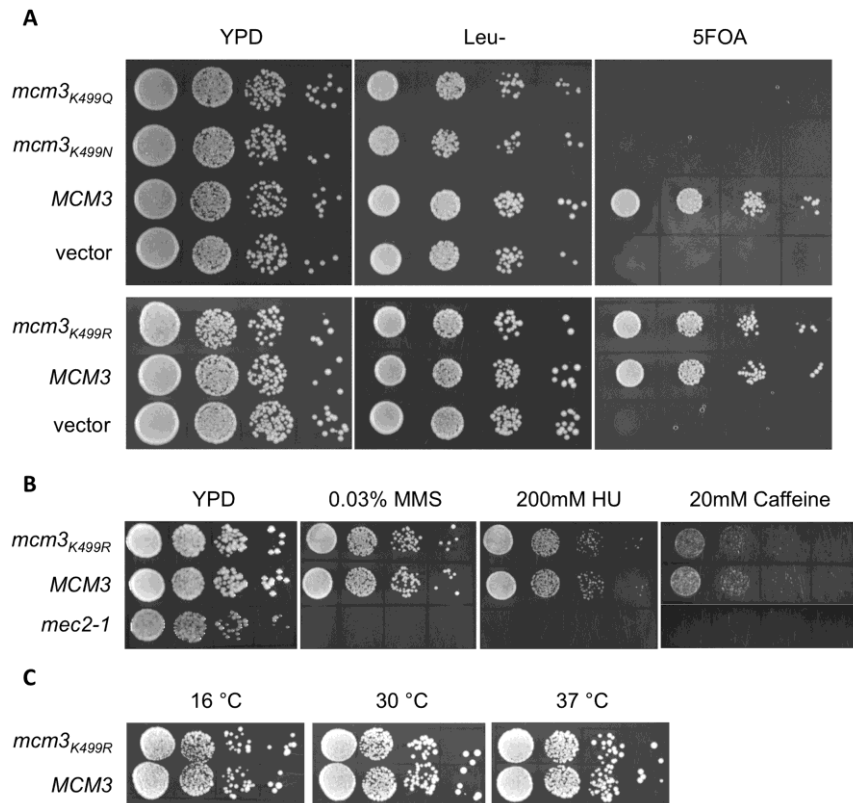
Figure 5. Characterization of *mcm3_{K499R}*, *mcm3_{K499N}*, and *mcm3_{K499Q}* alleles.

(A) The *MCM3*, *mcm3_{K499R}*, *mcm3_{K499N}*, and *mcm3_{K499Q}* genes encoded on *LEU2-*containing centromeric plasmids, or empty plasmid (vector), were transformed into MDY16 (*mcm3Δ* YCplac33-*MCM3*). The transformed yeast were grown overnight at 30°C in liquid YPD, serially diluted, and spotted onto YPD, synthetic complete lacking leucine, and YPD containing 5-FOA. (B) The *MCM3* and *mcm3_{K499R}* plasmid-shuffled strains were grown overnight at 30°C, serially diluted and spotted on YPD and YPD containing 0.03% MMS, 200 mM hydroxyurea (HU), or 20 mM caffeine. The *mec2-1* strain was subjected to the same growth assay as a positive control for genotoxic stress [51]. (C) The *MCM3* and *mcm3_{K499R}* plasmid-shuffled strains were grown overnight at 30°C, serially diluted, spotted on YPD, and grown at 16°C, 30°C or 37°C.

doi:10.1371/journal.pone.0082177.g005

To begin to investigate how Mcm3$_{K499A}$ disrupts function, we addressed whether its overexpression would have a dominant negative effect. A plasmid expressing *mcm3$_{K499A}$* or *MCM3* from a *GAL10* promoter was transformed into BY4741 (*MCM3*), and serial dilutions plated onto media containing glucose, raffinose, or galactose. In the presence of glucose or raffinose, where the *GAL10* promoter is transcriptionally repressed or not induced respectively, there was no effect on growth, whereas in galactose-containing media induction of *mcm3$_{K499A}$* expression resulted in a slow growth phenotype (Figure 6A). In addition, there was an increase of approximately three-fold in cell diameter for the *GAL10-mcm3$_{K499A}$* transformed strain compared to *GAL10-MCM3* transformed strain when grown in galactose-containing media (Figure 6B and 6C). Based on these observations, overexpression of *mcm3$_{K499A}$* in the context of a wild type background leads to a dominant negative effect that is likely associated with a cell cycle defect.
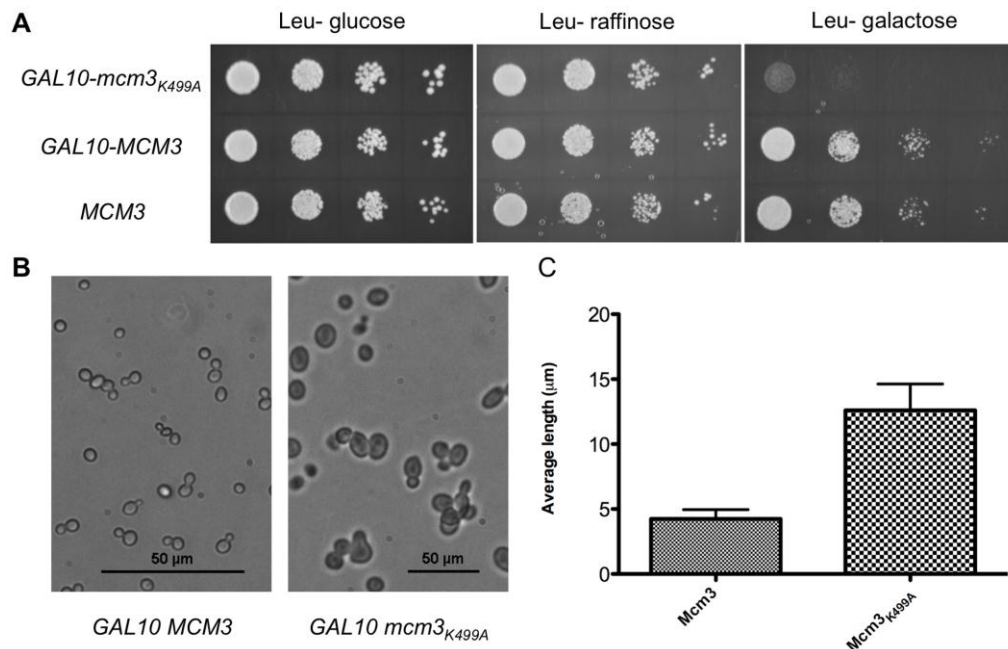
Figure 6. Effect of over-expressing the Mcm3$_{K499A}$ subunit in a wild-type background.

(A) BY4741 transformed with YCplac111-*GAL10-MCM3*, YCplac111-*GAL10-mcm3$_{K499A}$*, or YCplac111-*GAL10* were grown overnight in media with 2% raffinose lacking leucine, serially diluted, and spotted onto plates lacking leucine and containing 2% glucose, 2% raffinose, or 2% galactose. (B) BY4741 bearing YCplac111-*GAL10-MCM3* or YCplac111-*GAL10-mcm3$_{K499A}$* was grown in 2% galactose media lacking leucine and imaged using a Nikon Eclipse Ti microscope. Scale bars represent 50 µm. (C) The minimal diameter at the midsection was determined for BY4741 transformed with YCplac111-*GAL10-MCM3* or YCplac111-*GAL10-mcm3$_{K499A}$* grown as above. The average diameter for 20 cells for each strain is shown with the standard deviation indicated. doi:10.1371/journal.pone.0082177.g006

2.3.2 The Mcm3 PS1 β hairpin is required for DNA unwinding

To determine the biochemical effects of $Mcm3_{K499A}$ on the activity of the complex, we reconstituted it into Mcm2-7 to yield $Mcm2-7_{3K499A}$. Each of the subunits, including $Mcm3_{K499A}$ was expressed as a recombinant protein in E. coli, and checked for the absence of contaminating nuclease or ATPase activity. Individual Mcm subunits were mixed in equal molar ratios to reconstitute the hexameric complex, the final step of the reconstitution being elution from a gel filtration column. $Mcm2-7_{3K499A}$ eluted at a volume corresponding to the MCM hexamer, similar to wild-type Mcm2-7 (~600 kDa; Figure 7A). We examined the DNA unwinding of wild type and mutant Mcm complexes using a radiolabeled synthetic fork substrate where DNA unwinding is measured as the amount of single stranded DNA liberated from the duplex substrate. At a concentration of 200 nM the wild-type complex converted 1.5 fmoles of substrate to single-stranded DNA in 10 minutes (Figures 7B and 7C). By contrast, the 200 nM concentration of $Mcm2-7_{3K499A}$ unwound 0.1 fmol of the fork substrate. Therefore $Mcm2-7_{3K499A}$ has a, 15-fold reduction in helicase activity, indicating that the Mcm3 PS1 β hairpin is critical for DNA unwinding.
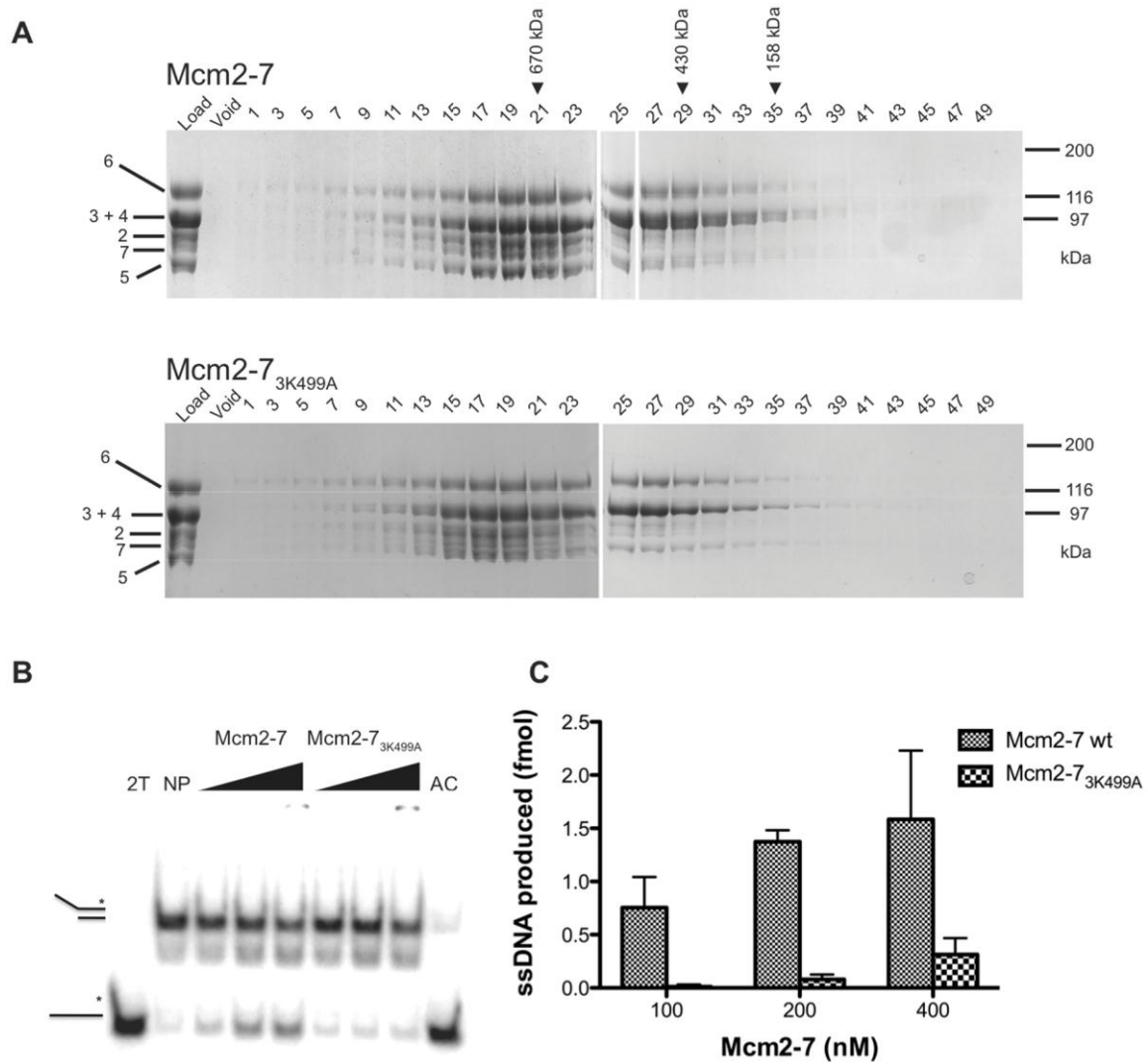
Figure 7. Reconstitution and analysis of Mcm2-7$_{3K499A}$.

(A) Individual Mcm subunits were expressed in bacteria, purified, and mixed in an equimolar ratio to reconstitute the hexameric complex. The Mcm2-7 complexes were then subjected to gel filtration chromatography, and fractions analyzed by SDS-PAGE. The top profile shows the wild-type Mcm2-7 complex, while the lower profile is the complex reconstituted with Mcm3$_{K499A}$. (B) A synthetic forked substrate radiolabeled on the 5′ end (indicated by the asterisk) was incubated with 100, 200, and 400 nM of either Mcm2-7 or Mcm2-7$_{3K499A}$ to assess the helicase activity of the reconstituted hexamers.

The "no protein" (NP) lane indicates the position of the radiolabeled substrate DNA, and a sample containing only radiolabeled single strand DNA (2T) was used to mark the location of the liberated single strand product. The inability of the two single strands to re-anneal is demonstrated in the last lane (AC); here, the complementary (non radiolabeled) strand was added to the radiolabeled (2T) strand at the start of the helicase assay. (C) The relative ability of Mcm2-7 and Mcm2-7$_{3K499A}$ to unwind DNA was quantitated by densitometric analysis of three replicates of the experiment shown in Panel B. doi:10.1371/journal.pone.0082177.g007

The loss of helicase activity in Mcm2-7$_{3K499A}$ may be due to a role for the Mcm3 PS1 hairpin in the ATPase activity of the complex. Interestingly, of the isolated dimer pairs, the pair of Mcm3 and Mcm7 has the highest ATPase activity, approaching that of the intact Mcm2-7 hexamer [25]. ATP hydrolysis was measured for intact wild-type Mcm2-7 and Mcm2-7$_{3K499A}$ complexes. As shown in Figure 8A, the ATP hydrolysis rate for Mcm2-7$_{3K499A}$ was not significantly different from the wild-type Mcm2-7. We next addressed whether Mcm2-7$_{3K499A}$ is capable of single-stranded DNA binding. Mutant and wild-type complexes were chromatographed on a single-stranded Sepharose affinity column in the presence of ATP, and eluted with increasing salt concentration. As shown in Figure 8B, wild type Mcm2-7 eluted from this column primarily in the 200 and 300 mM NaCl wash fractions (upper panel). The elution profile for Mcm2-7$_{3K499A}$ closely resembled that of the wild type complex (middle panel) indicating that the Mcm2-7$_{3K499A}$ is capable of binding single stranded DNA. Lack of binding by the peptidyl prolyl isomerase Pin-1 (lower panel), a relatively basic protein with a pI of 9.4, indicated that the binding by the Mcm complexes was specific for DNA and not simply due to charge interactions. We next used an electrophoretic mobility shift assay in an attempt to detect more subtle differences in DNA binding. A 59 radiolabeled oligonucle- otide of 90 bases was used as the substrate. As shown in Figure 8C (lanes 3–6) increasing concentrations of wild-type Mcm2-7 depleted the substrate band and resulted in the appearance of a discrete band of reduced mobility. To confirm that the band of slower mobility was a Mcm2-7-DNA complex, Mcm7 antibody was pre-incubated with Mcm2-7 prior to addition of radiolabeled oligonucleotide (Figure 8C lanes 7-10). In the presence of the antibody the band of slower mobility was diminished, indicating that it contained Mcm2-

7. When the DNA binding activity of Mcm2-7$_{3K499A}$ was assayed (lanes 11–14), the amount of Mcm2- 7$_{3K499A}$-DNA complex was reduced suggesting that Mcm2- 7$_{3K499A}$ is less able to bind the 90 base single-stranded DNA or that the binding is unstable under the electrophoresis conditions.
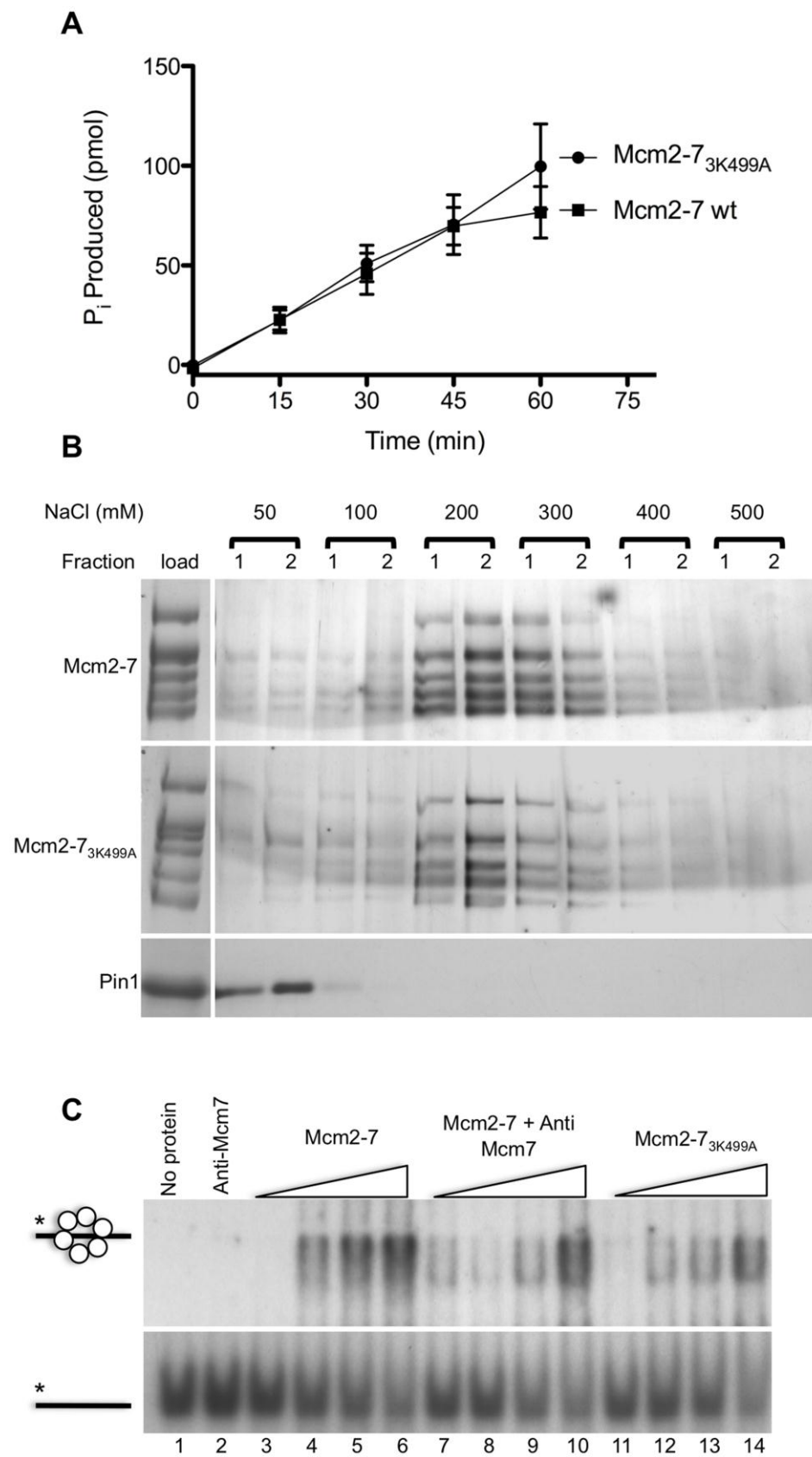
A

B

C

Figure 8. ATPase activity and DNA binding by Mcm2-7$_{3K499A}$.

(A) The reconstituted Mcm2-7 and Mcm2-7$_{3K499A}$ complexes were tested for ATPase activity by incubating with [γ^{32}P]-ATP and measuring the radioactivity of free Pi produced at the time points indicated. (B) Elution profile of Mcm2-7 and Mcm2-7$_{3K499A}$ from ssDNA-Sepharose. Five micrograms of Mcm2-7 (upper panel), Mcm2-7$_{3K499A}$ (middle panel), and the peptidyl prolyl isomerase Pin-1 (lower panel) were chromatographed on a 200 µL single-stranded DNA Sepharose column in the presence of 5 mM ATP. At each step the column was washed twice with 200 µL of buffer containing 50 mM, 100 mM, 200 mM, 300 mM, 400 mM, or 500 mM NaCl. Twenty-four microliters of each fraction was separated by SDS-PAGE (6%) and stained with colloidal blue to detect the load (left) and then silver stain to detect the fractions (right). (C) An electrophoretic mobility shift assay of DNA binding by Mcm2-7 (lanes 3-6) and Mcm2-7$_{3K499A}$ (lanes 11–14). 5′ radiolabeled ATGTCCTAGCAAGCCAGAATTCGGCAGCGTC(T)$_{60}$ was incubated with increasing concentrations (50, 100, 200, or 400 nM) of the Mcm hexameric complexes and separated in a 5% native polyacrylamide gel. Lanes 7-10 included a pre-incubation of the wild-type complex with an anti-Mcm7 antibody. Lanes 1 and 2 show the position of the DNA in the absence of protein, and in the presence of the anti-Mcm7 antibody, respectively. doi:10.1371/journal.pone.0082177.g008

The loss of helicase activity is the most pronounced functional effect of the Mcm3 hairpin mutation, and may explain the inviability of the *mcm3$_{K499A}$* strain. To investigate the effects of the Mcm3 hairpin mutation in cells, we analyzed myc[9]-Mcm3$_{K499A}$ expressed in yeast to determine if its ability to associate with other components required for replication differs from the wild type protein. Whole cell extracts containing myc9-tagged Mcm3 or Mcm3$_{K499A}$ were prepared from cells grown to mid-log phase in YPD media and analyzed by gel filtration chromatography on a Superose 6 column. As shown in Figure 9, wild type Mcm3 elutes from the Superose 6 column in two peaks. The first peak is broad and corresponds to complexes with a molecular mass greater than 2 MDa. We suspect that this may represent the Mcm2-7 complex associated with chromatin. The second peak elutes in the molecular mass range from 150 to 350 kDa. This likely represents Mcm3 in association with other molecules, and perhaps an equilibrium between subcomplexes of Mcms. The elution profile of myc[9]-Mcm3$_{K499A}$ resembled that of the wild type in that it eluted as two peaks, but with significant differences for the high- and low- molecular weight complexes. In the high molecular weight complex, Mcm3 appears as a single band that migrates with a mass of 135 kDa, while in the mcm3$_{K499A}$ strain, Mcm3 appears as a 135 kDa band but there are also two prominent bands at approximately 150 kDa and 175 kDa. These were not detected in the wild-type Mcm3 cells, even after prolonged exposure of the film. The reduced mobility forms of Mcm3 are likely the result of protein modification, but the nature of this modification is unclear. The second difference between wild-type and *mcm3$_{K499A}$* cells is that the smaller complex from wild-type cells elutes with a peak at 200 kDa (fraction 34 on the profile, Figure 9), which was shifted to approximately 260 kDa in the mcm3$_{K499A}$ strain (fraction

32). Since the purified Mcm2-7$_{3K499A}$ hexamer assembles and behaves similarly to the wild-type complex in vitro, these results suggest that in cells the altered activities of the Mcm2- 7$_{3K499A}$ complex result in changes in its molecular associations. Mcm3 has a unique role in the initiation process in that it is able to recruit its neighboring subunits, Mcm5 and Mcm7, to the origin recognition complex (ORC) independent of Cdt1 [44]. A winged helix domain only present at the C-terminal of Mcm3 interacts with the Cdc6/ORC complex to stimulate the ATP hydrolysis required for time-dependent stable double hexamer loading [45,46]. It may be that these processes are compromised by the poor helicase activity of Mcm3$_{K499A}$, leading to the differences we observe in Mcm3$_{K499A}$-containing complexes.
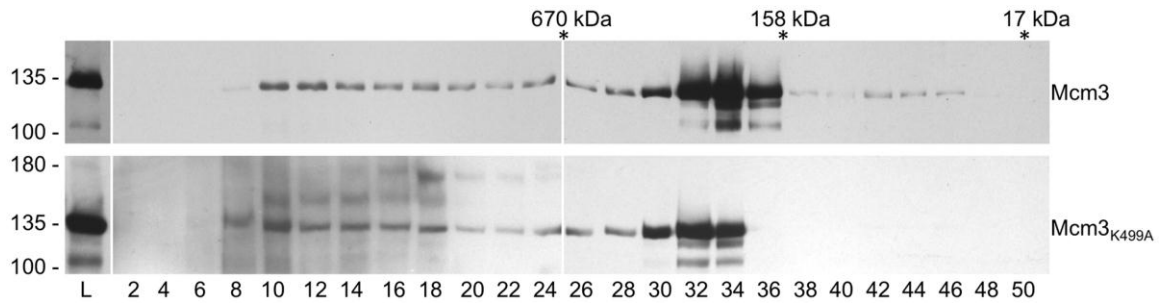
Figure 9. Analysis of myc[9]-tagged Mcm3 and Mcm3$_{K499A}$ by gel filtration.

Extracts were prepared from yeast strains MDY405 (myc[9]-Mcm3) and MDY406 (myc[9]-Mcm3$_{K499A}$). Five mg of protein was separated on a Superose 6HR10/30 column. Protein from 10 µL aliquots of 250 µL fractions for Mcm3 and 20 µL for Mcm3$_{K449A}$ were resolved by SDS-PAGE and myc-tagged protein detected by western blotting with anti-myc antibody. Fraction numbers are indicated below (L, load). The migration of molecular mass standards on the gel is shown on the left. The fractions corresponding to the peak elution of mass standards from the Superose 6 column is shown above.

doi:10.1371/journal.pone.0082177.g009

The observation that the Mcm3 PS1 hairpin is required for viability, while the PS1 β hairpins of the other five subunits are individually dispensable provides insight into possible mechanisms for DNA unwinding by Mcm2-7. To understand the role of the Mcm3 PS1 β hairpin, it is necessary to place it in the context of the Mcm2-7 hexamer, and to this end we modeled the structure of the Mcm2-7 complex using the structure of almost full-length SsoMCM monomer as a template for the individual Mcm2 through Mcm7 subunits; the hexameric structure of the N- terminal domain of *Methanobacterium thermoautotrophicum* MCM (mtMCM) was then used to assemble each of Mcm 2 through 7 into the hexameric Mcm2-7 complex (Figure 10A and 10B). Two interesting observations emerge from the Mcm2-7 model. First, the central channel exhibits a funnel-like shape, with the large opening formed by the C-terminal domains of the six subunits, and the smaller opening formed by the N-terminal domains. In fact, an extra domain in Mcm6 will further constrict the smaller N- terminal end of the Mcm2-7 hexamer. The Mcm6 domain comprises residues 407 to 475 and is inserted into a loop between two conserved b-strands in the SsoMCM and mtMCM structures; therefore its position inside the central channel is almost certain, although the degree to which it obstructs the central channel will depend on its structure, which has not been modeled. In addition to the funnel shape, the surface charge of the central channel exhibits a systematic change: the large opening formed by the C- terminal domains carries a negative surface charge, while the surface formed by the more constricted N-terminal domains is positively charged (Figure 10B).
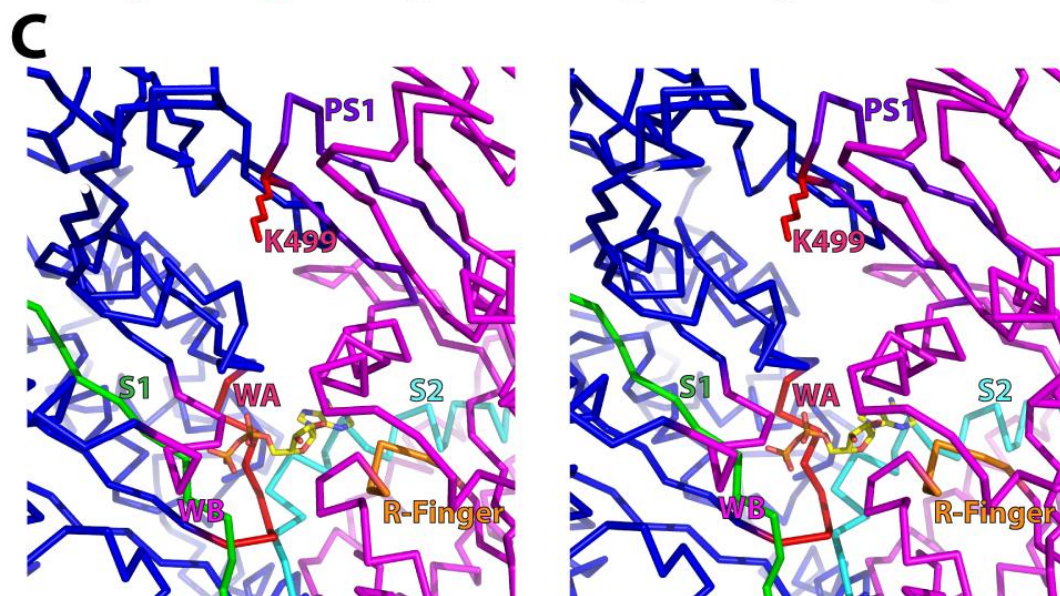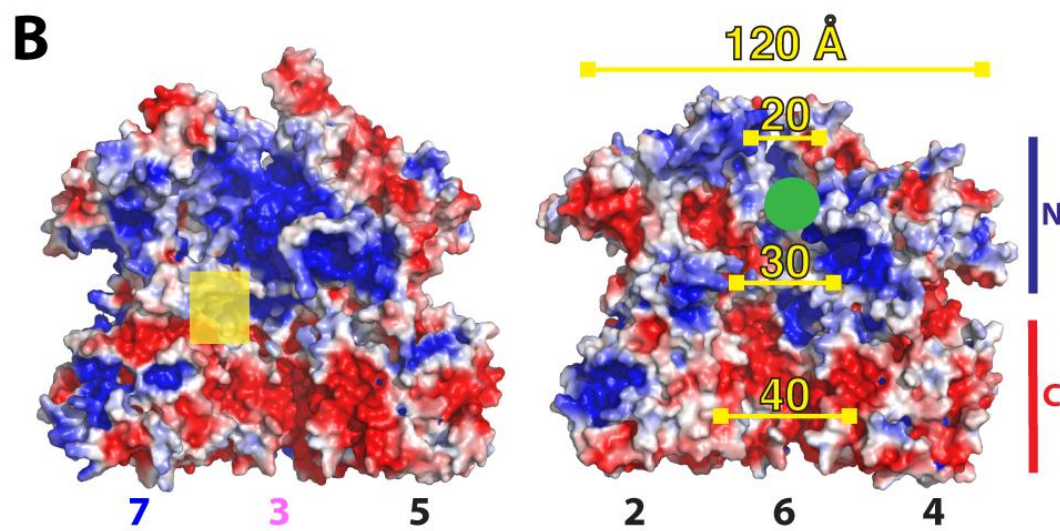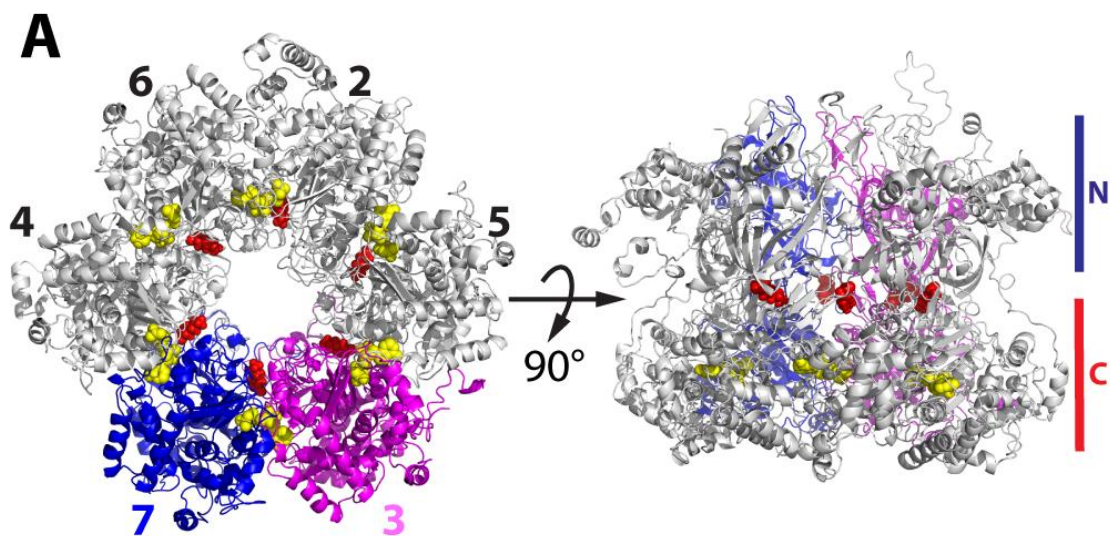
Figure 10. Model of Mcm2-7.

(A) Two views of the Mcm2-7 hexamer: on the left, looking through the central channel from the C-terminal end, and on the right, rotated 90° about a horizontal axis. The N- and C-terminal domains of the subunits are indicated. Subunits 3 and 7 are highlighted in magenta and blue, respectively, and the side chains of the PS1 lysyl residues are shown as space-filling models in red. ADP modeled onto the Walker A motifs is shown as a yellow space-filling model. (B) The hexamer is split into two halves - Mcm7/3/5 and Mcm2/6/4 - to show the electrostatic surface of the Mcm2-7 central channel; red indicates a negative surface potential, and blue a positive surface potential. The outer diameter of the hexamer is approximately 120 Å, while the inner diameter decreases from approximately 40 Å in the region formed by the C-terminal domains, to 20 Å or less in the region formed by the N-terminal domains. The N-terminal region will be further constricted by a 70-residue insertion in Mcm6, which is expected to occupy the region indicated with a green circle. A yellow square on the Mcm7/3/5 trimer indicates the potential side exit tunnel in the Mcm3/7 interface, which is shown in greater detail in Panel C. (C) Stereodiagram of the potential exit channel in the Mcm3/7 interface, illustrating the position of the Mcm3 PS1 hairpin (purple) and essential K499 residue (red) relative to ADP bound to Mcm7 and the motifs associated with ATP binding and hydrolysis: the Walker A (WA, red), Walker B (WB, magenta), and Sensor 1 (S1, green) of Mcm7, and the Arginine Finger (orange) and Sensor 2 (S2, cyan) of Mcm3.

doi:10.1371/journal.pone.0082177.g010

The second important observation from the Mcm2-7 model is that the PS1 β

hairpins of all Mcm subunits are somewhat recessed and do not project into the interior of

the central channel. Together with the reduced stability of DNA binding by Mcm2-

7_{3K499A}, these observations lead us to propose that the PS1 β hairpin may be a component

of an exit channel that directs one strand of incoming duplex DNA through the side of the

Mcm2-7 hexamer. A structural model of the SsoMCM hexamer suggests that side

channels are formed at the interface of subunits and run from the central channel to the

outside of the ring [7]; the side channels are wide enough to accommodate single-

stranded DNA. Similar channels are seen in electron micrographs of eukaryotic Mcm2-7

[47] and are present in our Mcm2-7 model (Figure 10C). The extrusion of single-stranded

DNA through a side channel of the Mcm2-7 complex is a possible explanation for

reduced helicase activity upon mutation of the Mcm3 PS1 β hairpin. Of note, the channel

incorporating the Mcm3 PS1 β hairpin is formed at the interface between Mcm3 and

Mcm7 (Figure 10C), which is critically important for Mcm2-7 function. For example,

when the various Mcm subunits are expressed independently to generate dimeric species,

it is the isolated Mcm3/7 dimer that has the highest ATPase activity, almost as high as the

ATPase of the intact Mcm2-7 hexamer [26,27]. Furthermore, expression of Mcm7 with

mutations in its Walker A or Walker B motif, or expression of Mcm3 with an R542A

mutation in its ''arginine finger'' lead to a strong dominant-lethal phenotype [26]. Taken

together, the shape and charge features of the Mcm2-7 ''funnel'', along with the

functional importance of catalytic components found in the Mcm3/7 interface, are

consistent with either double-stranded DNA or single-stranded DNA entering Mcm2-7 at

the larger C- terminal end. If double-stranded DNA enters the channel, it may be

destabilized due to the negative surface charge of the channel interior: one of the separated strands would be actively extruded through the Mcm3/7 interface, while the other strand could exit through the positively charged N-terminal end of the Mcm2-7 hexamer, or through another side channel. In a second possible scenario, single-stranded DNA would enter the Mcm2-7 channel and would be actively extruded through the Mcm3/7 interface, while the other strand would be sterically excluded from entering the channel.

The importance of the PS1 β hairpins in Mcm function is most apparent from the loss of viability when PS1 of Mcm3 was mutated. We demonstrate that the Mcm3 PS1 β hairpin participates in DNA unwinding by Mcm2-7, and based upon our in vitro experiments suggest that it may do so by altering the interaction of the complex with single-stranded DNA. This result is similar to findings with SsoMCM and the SF3 viral replicative helicases where the PS1 β hairpin is essential for helicase activity [8,9,48]. We also note that the interactions of $Mcm3_{K499A}$ are altered in cells as demonstrated by changes in its elution from a Superose 6 column. Whether these changes are due to or the cause of the defects in cellular function of the protein is unclear.

A key finding of our study is that of the six PS1 hairpins in the heterohexameric Mcm2-7 complex, only the PS1 β hairpin of Mcm3 is essential. This strongly suggests that it has a unique role in Mcm2-7 function. The finding that the PS1 β hairpin of Mcm3 is essential for viability is somewhat surprising since Mcm3 has been proposed to act principally in the regulation of the other Mcm2-7 subunits rather than have a direct role

in DNA unwinding [49,50]. Although not essential, the Mcm2, Mcm4, Mcm5, Mcm6 and Mcm7 PS1 hairpins are important for function as lysine to alanine mutations in any two subunits leads to inviability or slow growth. The finding that the $mcm4_{K658A}$ $mcm5_{K506A}$ double mutation strain was viable, in contrast to the lack of viability of other pairwise combinations is also another clear indication that each subunit contributes differently to the function of Mcm2-7.

2.4 Supporting Information
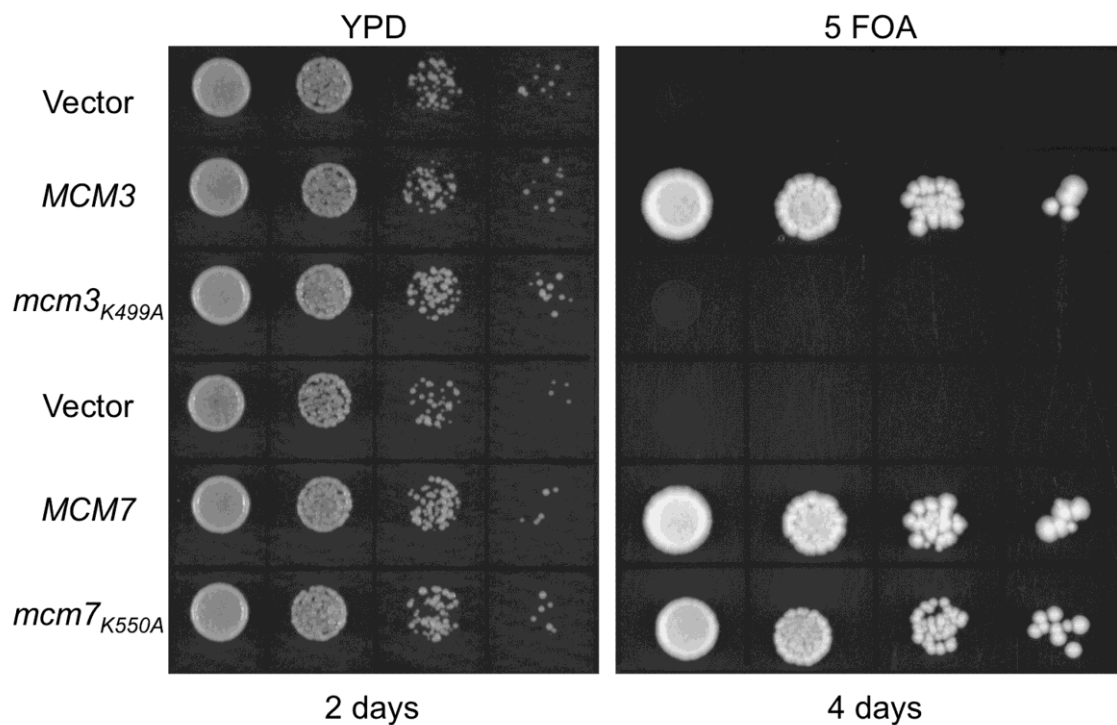
Figure S1. Growth of *mcm3_{K499A}* and *mcm7_{K550A}* plasmid shuffled yeast strains.

Haploid yeast strains deleted for *MCM3* or *MCM7* and bearing *MCM3* or *MCM7* on a *URA3-CEN* plasmid were transformed with *LEU2-CEN* plasmids containing either *MCM3*, *mcm3_{K499A}*, *MCM7*, *mcm7_{K550A}* or the empty *LEU2-CEN* plasmid (Vector). The transformed yeast were grown overnight at 30°C in YPD media, serially diluted, and then spotted onto a YPD plate or a plate containing 5-FOA. The plates were incubated at 30°C for the number of days indicated.
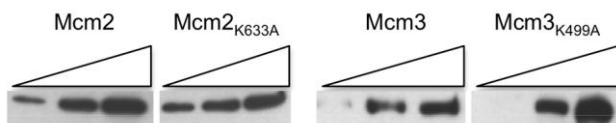
Figure S2. Expression levels of Mcm 2 and 3. Yeast strains MDY70 (MCM2), MDY71 (*mcm2$_{K633A}$*), MDY405 (*DED1-myc^9- MCM3*) and MDY406 (*DED1-myc^9-mcm3$_{K499A}$*) were grown to mid- log phase; yeast extracts were prepared by grinding with glass beads, and 10, 20 or 40 mg of total protein separated by SDS-PAGE. Blots of these gels were probed with anti-Mcm2, (Santa Cruz Biotech) or anti-myc (Sigma-Aldrich) antibody to assess the level of Mcm subunit. We note that for Mcm3 detection the plasmids were transformed into BY4741 and thus contain wild-type Mcm3.

2.5   Acknowledgments

We would like to thank Dr. David Edgell and Lance DaSilva for their comments on this project, Dr. Grant Brown for critically reading the manuscript, Dr. Bernard Duncker for strains, Michelle Dubinsky for Pin-1, and Ashley Miller, Tim Hatt and Atoosa Rezvanpour for technical assistance. This paper is dedicated to the memory of our late colleague, mentor, and friend Megan Davey.

2.6   Author Contributions

Conceived and designed the experiments: Megan J Davey, Christopher J Brandl, Brian H Shilton, Simon K W Lam. Performed the experiments: Megan J Davey, Christopher J Brandl, Brian H Shilton Simon K W Lam, Tina L Sing, Xiaoli Ma. Analyzed the data: Megan J Davey, Christopher J Brandl, Brian H Shilton, Simon K W Lam. Contributed reagents/materials/analysis tools: Megan J Davey, Christopher J Brandl, Brian H Shilton, Simon K W Lam, Tina L Sing, Xiaoli Ma. Wrote the paper: Megan J Davey, Christopher J Brandl, Brian H Shilton, Simon K W Lam.

2.7 Chapter 2 References

1. Bell SP, Dutta A (2002) DNA replication in eukaryotic cells. Annu Rev Biochem 71: 333–374.
2. Patel SS, Picha KM (2000) Structure and function of hexameric helicases. Annu Rev Biochem 69: 651–697.
3. Singleton MR, Dillingham MS, Wigley DB (2007) Structure and Mechanism of Helicases and Nucleic Acid Translocases. Annual Review of Biochemistry 76: 23–50.
4. Enemark EJ, Joshua-Tor L (2008) On helicases and other motor proteins. Curr Opin Struct Biol 18: 243–257.
5. Brewster AS, Chen XS (2010) Insights into the MCM functional mechanism: lessons learned from the archaeal MCM complex. Crit Rev Biochem Mol Biol 45: 243–256.
6. Kaplan DL, Davey MJ, O'Donnell M (2003) Mcm4,6,7 uses a "pump in ring" mechanism to unwind DNA by steric exclusion and actively translocate along a duplex. J Biol Chem 278: 49171–49182.
7. Brewster AS, Wang G, Yu X, Greenleaf WB, Carazo JM, et al. (2008) Crystal structure of a near-full-length archaeal MCM: functional insights for an AAA+ hexameric helicase. Proc Natl Acad Sci U S A 105: 20191–20196.
8. Enemark EJ, Joshua-Tor L (2006) Mechanism of DNA translocation in a replicative hexameric helicase. Nature 442: 270–275.
9. Gai D, Zhao R, Li D, Finkielstein CV, Chen XS (2004) Mechanisms of conformational change for a replicative hexameric helicase of SV40 large tumor antigen. Cell 119: 47–60.
10. Bae B, Chen YH, Costa A, Onesti S, Brunzelle JS, et al. (2009) Insights into the architecture of the replicative helicase from the structure of an archaeal MCM homolog. Structure 17: 211–222.
11. Enemark EJ, Joshua-Tor L (2006) Mechanism of DNA translocation in a replicative hexameric helicase. Nature 442: 270–275.
12. McGeoch AT, Trakselis MA, Laskey RA, Bell SD (2005) Organization of the archaeal MCM complex on DNA and implications for the helicase mechanism. Nat Struct Mol Biol 12: 756–762.
13. Bochman ML, Schwacha A (2009) The Mcm complex: unwinding the mechanism of a replicative helicase. Microbiol Mol Biol Rev 73: 652–683.
14. Forsburg SL (2004) Eukaryotic MCM proteins: beyond replication initiation. Microbiol Mol Biol Rev 68: 109–131.
15. Brown GW, Kelly TJ (1998) Purification of Hsk1, a minichromosome maintenance protein kinase from fission yeast. J Biol Chem 273: 22083–22090.
16. Bruck I, Kaplan D (2009) Dbf4-Cdc7 phosphorylation of Mcm2 is required for cell growth. J Biol Chem 284: 28823–28831.
17. Charych DH, Coyne M, Yabannavar A, Narberes J, Chow S, et al. (2008) Inhibition of Cdc7/Dbf4 kinase activity affects specific phosphorylation sites on MCM2 in cancer cells. J Cell Biochem 104: 1075–1086.
18. Chuang LC, Teixeira LK, Wohlschlegel JA, Henze M, Yates JR, et al. (2009) Phosphorylation of Mcm2 by Cdc7 promotes pre-replication complex assembly

during cell-cycle re-entry. Mol Cell 35: 206–216.

19. Lei M, Kawasaki Y, Young MR, Kihara M, Sugino A, et al. (1997) Mcm2 is a target of regulation by Cdc7-Dbf4 during the initiation of DNA synthesis. Genes Dev 11: 3365–3374.
20. Masai H, Taniyama C, Ogino K, Matsui E, Kakusho N, et al. (2006) Phosphorylation of MCM4 by Cdc7 kinase facilitates its interaction with Cdc45 on the chromatin. J Biol Chem 281: 39249–39261.
21. Montagnoli A, Valsasina B, Brotherton D, Troiani S, Rainoldi S, et al. (2006) Identification of Mcm2 phosphorylation sites by S-phase-regulating kinases. J Biol Chem 281: 10281–10290.
22. Sheu YJ, Stillman B (2006) Cdc7-Dbf4 phosphorylates MCM proteins via a docking site-mediated mechanism to promote S phase progression. Mol Cell 24: 101–113.
23. Sheu YJ, Stillman B (2010) The Dbf4-Cdc7 kinase promotes S phase by alleviating an inhibitory activity in Mcm4. Nature 463: 113–117.
24. Tsuji T, Ficarro SB, Jiang W (2006) Essential role of phosphorylation of MCM2 by Cdc7/Dbf4 in the initiation of DNA replication in mammalian cells. Mol Biol Cell 17: 4459–4472.
25. Stead BE, Brandl CJ, Davey MJ Phosphorylation of Mcm2 modulates Mcm2-7 activity and affects the cell's response to DNA damage. Nucleic Acids Res 39: 6998–7008.
26. Bochman ML, Bell SP, Schwacha A (2008) Subunit organization of Mcm2-7 and the unequal role of active sites in ATP hydrolysis and viability. Mol Cell Biol 28: 5865–5873.
27. Davey MJ, Indiani C, O'Donnell M (2003) Reconstitution of the Mcm2–7p heterohexamer, subunit arrangement, and ATP site architecture. J Biol Chem 278: 4491–4499.
28. Schwacha A, Bell SP (2001) Interactions between two catalytically distinct MCM subgroups are essential for coordinated ATP hydrolysis and DNA replication. Mol Cell 8: 1093–1104.
29. Forsburg SL, Sherman DA, Ottilie S, Yasuda JR, Hodson JA (1997) Mutational analysis of Cdc19p, a Schizosaccharomyces pombe MCM protein. Genetics 147: 1025–1041.
30. Bochman ML, Schwacha A (2008) The Mcm2-7 Complex Has In Vitro Helicase Activity. Molecular Cell 31: 287–293.
31. Stead BE, Sorbara CD, Brandl CJ, Davey MJ (2009) ATP Binding and Hydrolysis by Mcm2 Regulate DNA Binding by Mcm Complexes. Journal of Molecular Biology 391: 301–313.
32. Gietz RD, Sugino A (1988) New yeast-Escherichia coli shuttle vectors constructed with in vitro mutagenized yeast genes lacking six-base pair restriction sites. Gene 74: 527–534.
33. Hoke SM, Irina Mutiu A, Genereaux J, Kvas S, Buck M, et al. Mutational analysis of the C-terminal FATC domain of Saccharomyces cerevisiae Tra1. Curr Genet 56: 447–465.
34. Boeke JD, Trueheart J, Natsoulis G, Fink GR (1987) 5-Fluoroorotic acid as a selective agent in yeast molecular genetics. Methods Enzymol 154: 164–175.

35. Scherer S, Davis RW (1979) Replacement of chromosome segments with altered DNA sequences constructed in vitro. Proc Natl Acad Sci U S A 76: 4951–4955.
36. Mutiu AI, Hoke SM, Genereaux J, Hannam C, MacKenzie K, et al. (2007) Structure/function analysis of the phosphatidylinositol-3-kinase domain of yeast tra1. Genetics 177: 151–166.
37. Saleh A, Lang V, Cook R, Brandl CJ (1997) Identification of native complexes containing the yeast coactivator/repressor proteins NGG1/ADA3 and ADA2. J Biol Chem 272: 5571–5578.
38. Chivian D, Baker D (2006) Homology modeling using parametric alignment ensemble generation with consensus and energy-based model selection. Nucleic Acids Res 34: e112.
39. Raman S, Vernon R, Thompson J, Tyka M, Sadreyev R, et al. (2009) Structure prediction for CASP8 with all-atom refinement using Rosetta. Proteins 77 Suppl 9: 89–99.
40. Fletcher RJ, Bishop BE, Leon RP, Sclafani RA, Ogata CM, et al. (2003) The structure and function of MCM from archaeal *M. Thermoautotrophicum*. Nat Struct Biol 10: 160–167.
41. Dolinsky TJ, Nielsen JE, McCammon JA, Baker NA (2004) PDB2PQR: an automated pipeline for the setup of Poisson-Boltzmann electrostatics calcula- tions. Nucleic Acids Res 32: W665–667.
42. Baker NA, Sept D, Joseph S, Holst MJ, McCammon JA (2001) Electrostatics of nanosystems: application to microtubules and the ribosome. Proc Natl Acad Sci U S A 98: 10037–10041.
43. Maine GT, Sinha P, Tye BK (1984) Mutants of S. cerevisiae defective in the maintenance of minichromosomes. Genetics 106: 365–385.
44. Moreau MJ, McGeoch AT, Lowe AR, Itzhaki LS, Bell SD (2007) ATPase site architecture and helicase mechanism of an archaeal MCM. Mol Cell 28: 304– 314.
45. Frigola J, Remus D, Mehanna A, Diffley JF ATPase-dependent quality control of DNA replication origin licensing. (2013) Nature 495: 339–343.
46. Fernandez-Cid A, Riera A, Tognetti S, Herrera MC, Samel S, et al. An ORC/ Cdc6/MCM2-7 complex is formed in a multistep reaction to serve as a platform for MCM double-hexamer assembly. (2013) Mol Cell 50: 577–588.
47. Remus D, Beuron F, Tolun G, Griffith JD, Morris EP, et al. (2009) Concerted loading of Mcm2-7 double hexamers around DNA during DNA replication origin licensing. Cell 139: 719–730.
48. McGeoch AT, Trakselis MA, Laskey RA, Bell SD (2005) Organization of the archaeal MCM complex on DNA and implications for the helicase mechanism. Nat Struct Mol Biol 12: 756–762.
49. Lee JK, Hurwitz J (2000) Isolation and characterization of various complexes of the minichromosome maintenance proteins of Schizosaccharomyces pombe. J Biol Chem 275: 18871–18878.
50. Tye BK, Sawyer S (2000) The Hexameric Eukaryotic MCM Helicase: Building Symmetry from Nonidentical Parts. J Biol Chem 275: 34833–34836.
51. Weinert TA, Kiser GL, Hartwell LH (1994) Mitotic checkpoint genes in budding yeast and the dependence of mitosis on DNA replication and repair. Genes & Development 8: 652–665.

52. Winzeler EA, Davis RW (1997) Functional analysis of the yeast genome. Curr Opin Genet Dev 7: 771–776.

CHAPTER 3: DISCUSSION

3.1   General discussion.

Mcm2-7 is the putative replicative helicase in eukaryotes. All six subunits are required for the initiation and progression of DNA replication [1]. As a critical component of the replisome, Mcm2-7 is a target of various intra S phase checkpoint kinases implicating its importance in genomic stability [2,3]. Although the general architecture of the Mcm2-7 complex is a ring structure similar to other hexameric helicases, currently there are no molecular structures solved for the eukaryotic Mcm2-7. Due to the high protein sequence conservation between Mcm2-7, archaeal MCMs, and viral helicases, structural features identified in the prokaryotic and viral helicases should also be present Mcm2-7. Therefore, structure/function studies of Mcm2-7 have been modeled on the crystal structures of archaeal MCMs and viral hexameric helicases. The canonical AAA+ domain found in all archaeal MCMs, viral hexmaeric helicases, and Mcm2-7 contain the Walker A, Walker B, and arginine finger motifs that are required for ATP binding and hydrolysis. In addition, four hairpins have been discovered in archaeal MCMs and mutational studies show that these hairpins are important for the proper functioning of the helicase.

In this thesis, *in vitro* analysis of the Mcm2-7$_{3K499A}$ has shown that ATPase is not affected by mutation of the PS1 β hairpin. Furthermore, the presence of ATPase activity

similar to the wild type level suggests that the hexameric complex has not been disrupted by a PS1 β hairpin mutation as functional ATPase sites require that adjacent Mcm subunits interact with one another to bind and hydrolyze ATP. The stability of the Mcm2-7_{3K499A} was further confirmed by gel filtration. These findings were similar to studies of Sso MCM PS1 β hairpins [4].   However, there was a subtle loss of DNA binding suggesting that the PS1 β hairpin is more directly involved in DNA unwinding. These experimental results are similar to Sso MCM studies [4]. Structural data gathered from the E1 helicase indicates the PS1 β hairpin makes contact with the sugar phosphate backbone of DNA [5]. Furthermore, in order to translocate and unwind DNA efficiently, Mcm2-7 is thought to bind non-discriminately to DNA and transiently. Hence, the subtle loss of DNA binding in the Mcm2-7_{3K499A} complex may be explained by two factors; one being the loss of only one PS1 β hairpin contacting DNA and the other due to the non discriminate nature of DNA binding by Mcm2-7.

3.2   How is ATP-dependent DNA unwinding coordinated in Mcm2-7?

Three models for ATP coordinated DNA unwinding in hexameric helicases were previously discussed. The step wise model postulates that a single ATP hydrolysis event at each helicase subunit moves the nucleic acid strand one nucleotide at a time. In the concerted model all the helicase subunits would bind to ATP and hydrolyze at the same time to drive DNA unwinding. In the semi-sequential model, only a subset of helicase subunits would be required to drive DNA unwinding. Since mutation of any two Mcm subunits' PS1 β hairpin results in synthetic lethality with the exception of the double $mcm4_{K658A}$ and $mcm5_{K506A}$ a semi-sequential model of ATP-dependent coordinated DNA

translocation and unwinding is likely utilized by Mcm2-7. In the $mcm4_{K658A}$ and $mcm5_{K506A}$ viable double mutant it becomes apparent that the most active ATPase dimer pairs, Mcm3/7 and Mcm2/6 are minimally required for viability. Furthermore, it is interesting to note that Mcm4 and Mcm5 are directly opposite of one another (Chapter 1, Figure 3). This suggests that movement and unwinding of DNA through the Mcm2-7 ring requires communication and effort from two opposite pairs of Mcm subunits working in unison. This is similar in manner to DnaB, the replicative helicase of prokaryotes. Recently, a hand over hand model was proposed to describe the mechanism by which ATP coordinated DNA translocation and unwinding in the DnaB hexameric helicase. In the hand over hand model, the subunits of DnaB work in pairs to move 2 nucleotides of DNA through the central channel during each ATP hydrolysis event; analogous to climbing a rope [6]. In DnaB, three identical dimers work together to move DNA through the ring, however in Mcm2-7 perhaps only the most active ATPase dimers Mcm3/7 and Mcm2/6 are involved in DNA translocation since the other dimers do not hydrolyze ATP at appreciable levels to provide the necessary mechanical force to move DNA.

3.3   Hierarchy of PS1 hairpins in Mcm2-7?

Genetic analysis of the Mcm2-7 PS1 β hairpins provides evidence that the Mcm3 and Mcm7 PS1 β hairpins play a greater role in translocation than the hairpins of other subunits. The $mcm3_{K499A}$ is inviable, and the $mcm7_{K550A}$ grows slower than the wild type strain in contrast to the other Mcm mutants which do not display any overt growth defects. In addition, Mcm4 and Mcm5 PS1 β hairpins may contribute the least to translocation as the synthetic lethal experiments showed that of the possible pair wise

combinations, only the $mcm4_{K658A}$ and $mcm5_{K506A}$ supports viability, albeit it grows more slowly than the single mutants and wild type strains. Mcm2-7 is an energy dependent motor and in order to translocate along DNA, chemical energy in the form of ATP is converted to mechanical energy. Intriguingly, the results gathered from genetic mutation of the PS1 β hairpin can be explained by pairwise ATPase studies of Mcm subunits. In pairwise studies of eukaryotic Mcm subunits, the most active ATPase site is located at the Mcm3/7 site; its activity approaches that of the Mcm2-7 complex levels and this correlates with the most disruptive PS1 β hairpin mutations located at $mcm3_{K499A}$ and $mcm7_{K550A}$ .This supports the view that the Mcm3 and Mcm7 PS1 β hairpins contribute the most in DNA translocation and unwinding. In contrast the Mcm2/5 and Mcm4/6 pairs do not display any appreciable level of ATPase, and a PS1 double mutant strain is viable when *MCM4* and *MCM5* are mutated. A possible model has most of the mechanical work performed by the Mcm3/7 pair where the PS1 β hairpin of Mcm3 and Mcm7 would provide the driving force to move the Mcm-7 along the DNA template, while the PS1 β hairpins of other Mcm subunits hold the DNA template temporarily in place during each translocation cycle to prevent slippage.

3.4   Why is the Mcm3 PS1 hairpin is essential?

Three general models for DNA translocation have been proposed for Mcm2-7. The steric exclusion model, where a single strand of DNA is threaded through the central channel of the helicase and the complementary strand is passively unwound outside of the helicase. The plowshare model, where the double helix enters the central channel and gets split physically by a "wedge" and the separated strands exit either through side

channels or the N – terminus. Lastly, the strand extrusion model where double stranded DNA enters the central channel and one strand is extruded through a side channel while the other strand exits through the N - terminus. Since the PS1 β hairpins are recessed and located near the side channels, the essential nature for the Mcm3 PS1 β hairpin is to actively direct the single stranded template through a side channel. In the structural Mcm2-7 model presented in Chapter 2, the Mcm6 subunit contains additional residues that would constrict the N-terminal end of the Mcm2-7 channel. This suggests that another exit point needs to be utilized by the separated DNA templates. As previously discussed, Mcm3/7 forms the most active ATPase site and would provide the necessary chemo-mechanical energy to the PS1 β hairpin of Mcm3 to facilitate DNA through the side channel. It is important to note in the Mcm2-7$_{3K499A}$ complex, ATPase is not affected when compared to a wild type complex *in vitro* suggesting the PS1 β hairpin mutation does not affect the ability to hydrolyze ATP at the Mcm3$_{K499A}$/Mcm7 dimer interface.

An *in vivo* approach I took to determine whether the Mcm2-7 PS1 β hairpins are involved in DNA translocation was to analyze the *mcm* mutants using florescence activated cell sorting (FACS) to measure the DNA content of the cell. One would expect that upon G1 release, the *mcm* mutants would replicate more slowly and contain less DNA than the wild type strain during timed measurements. However, this was not observed due to the fact yeast contain thousands of origins of replication and are able to recruit late firing origins to complete DNA replication in the event of slowed DNA replication. With the *mcm7$_{K550A}$* plasmid shuffled strain, I was able to detect a delay in S

phase progress. However, this may be due to plasmid stability issues since Mcm

mutations can disrupt plasmid maintenance in cells.

3.5   Significance

Based on models of the archaeal MCM, the PS1 β hairpin is predicted to be

involved in DNA translocation [4]. The findings of this thesis also implicate the PS1 β

hairpin as crucial component of DNA translocation and unwinding. Unlike the PS1 β

hairpin of archael MCM, each PS1 hairpin in Mcm2-7 does not contribute equally to its

function. This is most obvious in the mutational studies, and synthetic lethality tests

performed in this thesis. These observations are also consistent with the prevailing

thought that each subunit is unique in the eukaryotic replicative helicase.

3.6   Future directions

Chromatin immunoprecipitation (ChIP) would be an alternative approach to

examine whether PS1 β hairpins of Mcm2-7 are important for DNA translocation *in vivo*.

DNA-protein cross-links can be captured by formaldehyde treating of G1 released cells.

Mcm PS1 β hairpin mutants can then be immunoprecipitated and the amount of

replication fork progression measured indirectly by amplifying the DNA adjacent to the

fork that precipitates with the Mcm subunits.

Substantial technological advances have been made in the field of single molecule

studies that has provided a means to measure ultrasensitive protein-DNA dynamics. A

key advantage of single molecule experiments is the possibility to analyze particle

tracking of highly processive motor proteins that frequently participate in DNA replication, and transcription providing information at the base pair level [7]. One such study observed the dynamics of how the bacteriophage T7 gene product 4 hexameric helicase translocates along the DNA using single molecule methods and provided valuable mechanistic insights into how hexameric helicases translocate and unwind DNA [8]. In the study mentioned, Sun *et al*. were able to determine unwinding at the base pair level, slippage when the helicase was no longer able to hold tightly to the unwound DNA, as well as processivity of the helicase. Given that Mcm2-7 can be purified and loaded onto DNA *in vitro*, we can now utilize single molecule methods to interrogate how mutation of the PS1 β hairpin in Mcm2-7 affects its ability to translocate and unwind DNA at a higher resolution not previously achievable as our findings have already shown mutation of a different Mcm's PS1 β hairpin affects the function of the Mcm2-7 differently.

3.7 Chapter 3 References

1. Labib, K., Tercero, J.A., and Diffley, J.F. (2000) Uninterrupted MCM2-7 function required for DNA replication fork progression. *Science.* **288,** 1643-1647
2. Forsburg, S.L. (2008) The MCM helicase: linking checkpoints to the replication fork. *Biochem.Soc.Trans.* **36,** 114-119
3. Forsburg, S.L. (2004) Eukaryotic MCM proteins: beyond replication initiation. *Microbiol.Mol.Biol.Rev.* **68,** 109-131
4. McGeoch, A.T., Trakselis, M.A., Laskey, R.A., and Bell, S.D. (2005) Organization of the archaeal MCM complex on DNA and implications for the helicase mechanism. *Nat.Struct.Mol.Biol.* **12,** 756-762
5. Enemark, E.J., and Joshua-Tor, L. (2006) Mechanism of DNA translocation in a replicative hexameric helicase. *Nature.* **442,** 270-275
6. Itsathitphaisarn, O., Wing, R.A., Eliason, W.K., Wang, J., and Steitz, T.A. (2012) The hexameric helicase DnaB adopts a nonplanar conformation during translocation. *Cell.* **151,** 267-277
7. Robison, A.D., and Finkelstein, I.J. (2014) High-throughput single-molecule studies of protein-DNA interactions. *FEBS Lett.*
8. Sun, B., Johnson, D.S., Patel, G., Smith, B.Y., Pandey, M., Patel, S.S., and Wang, M.D. (2011) ATP-induced helicase slippage reveals highly coordinated subunits. *Nature.* **478,** 132-135

CURRICULUM VITAE

Simon Kai Wing Lam

EDUCATION:

2014 Master of Biochemistry, University of Western Ontario
2009 Honors Bachelor in Biochemistry, University of Western Ontario
2007 Bachelor of Science, Specialization in Pharmacology, University of Alberta
2005 Bachelor of Science in Biological Sciences and Chemistry, University of Alberta

ACADEMIC HONOURS, SCHOLARSHIPS, AND AWARDS:

1. Dean's Honour List (2006 – 2009)

2. Jason Lang Scholarship (2006 and 2007)

3. Alexander Rutherford Scholarship (1997 - 2000)

RESEARCH HONOURS, SCHOLARSHIPS, AND AWARDS:

1. American Society for Biochemistry and Molecular Biology (ASBMB) - Merit Award. Experimental Biology Meeting. Boston MA. 2013

2. American Society for Biochemistry and Molecular Biology (ASBMB) - Travel Award. Experimental Biology Meeting. Boston MA. 2013

3. University of Western Ontario Graduate Thesis Research Award. (2012 and 2013)

4. Western Graduate Research Scholarship. (2009 to 2013)

PUBLICATIONS, PRESENTATIONS AND ABSTRACTS:

1. <u>Simon K.W. Lam</u>, Xiaoli Ma, Tina L. Sing, Brian H. Shilton, Christopher J. Brandl, and Megan J. Davey. The PS1 hairpin of Mcm3 is essential for viability and for DNA unwinding *in vitro*. (2013) PlosOne.

2. <u>Simon K.W. Lam</u>, Tina L. Sing, Christopher J. Brandl, and Megan J. Davey. Investigation of the pre-sensor 1 hairpin in minichromosome maintenance proteins 2-7. American Society for Biochemistry and Molecular Biology. Experimental Biology Meeting. Boston, MA. 2013 (Poster presentation)

3. <u>Simon K.W. Lam</u>, Tina L. Sing, Christopher J. Brandl, and Megan J. Davey. The mechanism of DNA unwinding by the eukaryotic replicative helicase. Yeast Genetics and Molecular Biology Meeting. Princeton, NJ. 2012 (Poster presentation)

4. <u>Simon K.W. Lam</u>, Tina L. Sing, Christopher J. Brandl, and Megan J. Davey. Mutation of putative b hairpin disrupts minichromosome maintenance 2-7 function. Buffalo Symposium on Genomic Integrity and Disease. Buffalo, NY. 2011 (Poster presentation)

5. <u>Simon K.W. Lam</u>, Tina L. Sing, Christopher J. Brandl, and Megan J. Davey. Genetic analysis of beta hairpins in the function of Mcm2-7. Northeast Regional Yeast Meeting. Buffalo, NY. 2010 (Poster presentation)

6. <u>Simon K.W. Lam</u>, Tina L. Sing, Christopher J. Brandl, and Megan J. Davey. Genetic analysis of beta hairpins in the function of Mcm2-7. Buffalo DNA replication and Repair Meeting. Buffalo, NY. 2010 (Poster presentation)

RESEARCH EXPERIENCE:

2012 – 2013 Graduate Student
Department of Biochemistry
University of Western Ontario, London Ontario.
Supervisor: Christopher Brandl

2009 – 2012 Graduate Student
Department of Biochemistry
University of Western Ontario. London, Ontario.
Supervisor: Megan J. Davey (Deceased)

2007 Summer Research Student
Cross Cancer Institute. Edmonton, Alberta.
Supervisor: Roseline Godbout

TEACHING EXPERIENCE:

2010 – 2013 Teaching Assistant
Clinical Biochemistry 3386 and Introductory Biochemistry 2210.
University of Western Ontario. London, Ontario.